Click Here for Full Article

Characterizing the seismogenic zone of a major plate boundary subduction thrust: Hikurangi Margin, New Zealand

Laura M. Wallace, Martin Reyners, Ursula Cochran, and Stephen Bannister
GNS Science, P.O. Box 30368, Lower Hutt 5040, New Zealand (l.wallace@gns.cri.nz)

Philip M. Barnes
National Institute of Water and Atmospheric Research, P.O. Box 14901, Wellington 6021, New Zealand

Kelvin Berryman, Gaye Downes, and Donna Eberhart-Phillips
GNS Science, P.O. Box 30368, Lower Hutt 5040, New Zealand

Ake Fagereng
Department of Geology, University of Otago, P.O. Box 56, Dunedin 9054, New Zealand

Susan Ellis and Andrew Nicol
GNS Science, P.O. Box 30368, Lower Hutt 5040, New Zealand

Robert McCaffrey
GNS Science, P.O. Box 30368, Lower Hutt 5040, New Zealand

Now at Department of Earth and Environmental Science, Rensselaer Polytechnic Institute, Troy, New York 12180, USA

R. John Beavan, Stuart Henrys, Rupert Sutherland, Daniel H. N. Barker, and Nicola Litchfield
GNS Science, P.O. Box 30368, Lower Hutt 5040, New Zealand

John Townend
Institute of Geophysics, Victoria University of Wellington, P.O. Box 600, Wellington 6140, New Zealand

Russell Robinson, Rebecca Bell, Kate Wilson, and William Power
GNS Science, P.O. Box 30368, Lower Hutt 5040, New Zealand

[1] The Hikurangi subduction margin, New Zealand, has not experienced any significant ($>M_w$ 7.2) subduction interface earthquakes since historical records began ∼170 years ago. Geological data in parts of the North Island provide evidence for possible prehistoric great subduction earthquakes. Determining the seismogenic potential of the subduction interface, and possible resulting tsunami, is critical for estimating seismic hazard in the North Island of New Zealand. Despite the lack of confirmed historical interface events, recent geodetic and seismological results reveal that a large area of the interface is interseismically coupled, along which stress could be released in great earthquakes. We review existing geophysical and geological data in order to characterize the seismogenic zone of the Hikurangi subduction interface. Deep interseismic coupling of the southern portion of the Hikurangi interface is well defined by interpretation of

GPS velocities, the locations of slow slip events, and the hypocenters of moderate to large historical earthquakes. Interseismic coupling is shallower on the northern and central portion of the Hikurangi subduction thrust. The spatial extent of the likely seismogenic zone at the Hikurangi margin cannot be easily explained by one or two simple parameters. Instead, a complex interplay between upper and lower plate structure, subducting sediment, thermal effects, regional tectonic stress regime, and fluid pressures probably controls the extent of the subduction thrust's seismogenic zone.

1. Introduction

[2] Subduction zones have produced the largest and some of the most damaging earthquakes in historical times, most notably the 26 December 2004 Sumatra earthquake (M_w 9.2) and resulting tsunami. Detailed knowledge of where subduction megathrusts rupture in earthquakes (and where they do not) is critical for understanding the hazards associated with subduction megathrust events, and the physical processes behind subduction zone seismogenesis. Many investigators have attempted to explain the occurrence of subduction thrust earthquakes by correlating their size/frequency with certain parameters, such as subduction rate, subducting plate age, subduction interface thermal structure, or the presence of subducting sediment [e.g., *Uyeda and Kanamori*, 1979; *Ruff and Kanamori*, 1980; *Peterson and Seno*, 1984; *Kanamori*, 1986; *Ruff*, 1989; *Scholz and Campos*, 1995; *McCaffrey*, 1997]. However, the 2004 Sumatra earthquake challenged some of those conclusions regarding the physical controls on great (>M_w 8.0) subduction earthquakes [e.g., *Subarya et al.*, 2006; *Stein and Okal*, 2007; *McCaffrey*, 2007], reminding us that our comprehension of processes governing subduction zone seismogenesis is far from complete.

[3] At the Hikurangi subduction margin, New Zealand, significant progress has been made over the last decade in our understanding of the seismogenic potential and tectonics of the megathrust (Figure 1) [e.g., *Berryman*, 1993; *Barnes and Mercier de Lepinay*, 1997; *Barnes et al.*, 1998a; *Reyners*, 1998; *Webb and Anderson*, 1998; *Eberhart-*

Phillips and Reyners, 1999; *Darby and Beavan*, 2001; *Nicol and Beavan*, 2003; *Wallace et al.*, 2004; *Douglas et al.*, 2005; *Eberhart-Phillips et al.*, 2005; *Cochran et al.*, 2006; *Henrys et al.*, 2006; *Reyners et al.*, 2006; *Wallace and Beavan*, 2006; *Litchfield et al.*, 2007; *Barker et al.*, 2009; *Barnes et al.*, 2009]. However, because of the lack of historical Hikurangi subduction thrust earthquakes larger than M_w 7.2, our knowledge of its potential to rupture over large areas must be based on less direct evidence. Given the recent advances in our knowledge of the seismic behaviour and tectonics of the Hikurangi subduction margin, it is timely to synthesize these studies to better understand the geometry and nature of the seismogenic zone (the region where earthquakes can nucleate and rupture).

[4] We find that there are marked along-strike changes in the geometry of the likely seismogenic zone that correlate with major along-strike changes in a number of physical properties at the Hikurangi margin. However, the along-strike changes in the geometry of the seismogenic zone of the Hikurangi subduction thrust cannot be explained using only one or two simple parameters (such as temperature or sediment subduction), but probably require a complex interplay between factors such as upper plate and lower plate composition and structure, regional tectonic stress state, presence of subducted sediment, temperature of the interface, and the presence of fluids, among others. Despite this complexity, we suggest that improved data may lead to a relatively simple physical model that is
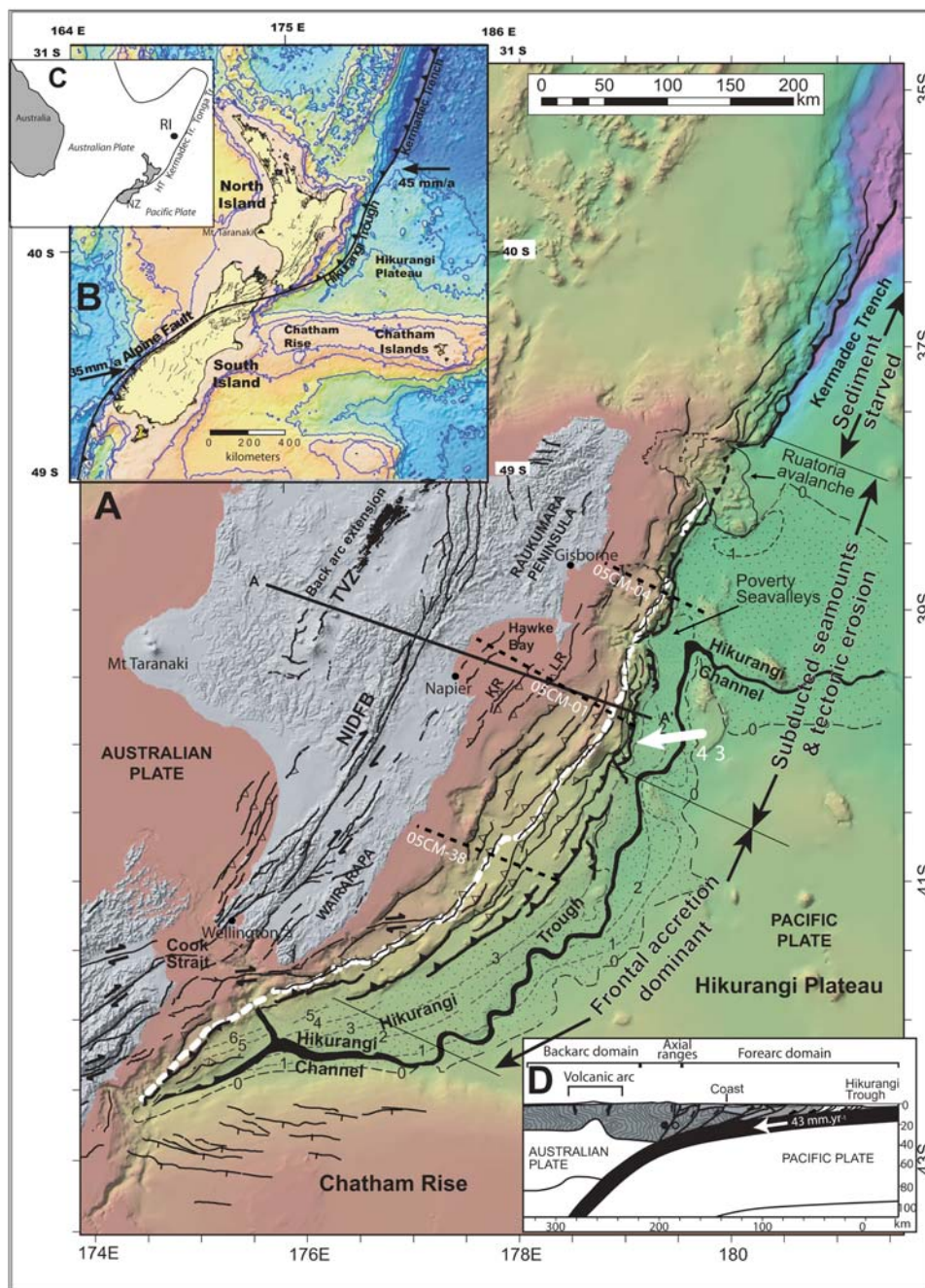
Figure 1. Tectonic setting of the Hikurangi margin. Modified from *Barnes et al.* [2009], copyright 2009, Elsevier. (a) Detailed bathymetry (NIWA), topography, and active faulting (black lines) of the onshore and offshore subduction margin. Dashed contours indicate sediment thickness on lower plate from *Lewis et al.* [1998]. Bold white dashed line shows the back of the accretionary wedge and the front of a deforming buttress of Cretaceous and Paleogene rocks covered by Miocene to Recent slope basins [from *Lewis et al.*, 1997; *Barnes et al.*, 1998b, 2009]. A−A′ line denotes cross-section location in Figure 1d. Dashed black lines show locations of seismic reflection lines from Figure 4, labeled by line number. White arrow shows Pacific/Australia relative plate motion in the region from *Beavan et al.* [2002]. Onshore active faults from GNS Science active faults database (http://maps.gns.cri.nz/website/af/). TVZ, Taupo Volcanic Zone; NIDFB, North Island Dextral Fault Belt; LR, approximate location of Lachlan Ridge; KR, approximate location of Kidnappers Ridge. (b) Broader-scale New Zealand tectonic setting. (c) Regional tectonic framework. RI, Raoul Island; NZ, New Zealand; HT, Hikurangi Trough. (d) Interpretive cross section across the strike of the subduction margin. Cross-section location denoted by A−A′ line in Figure 1a.
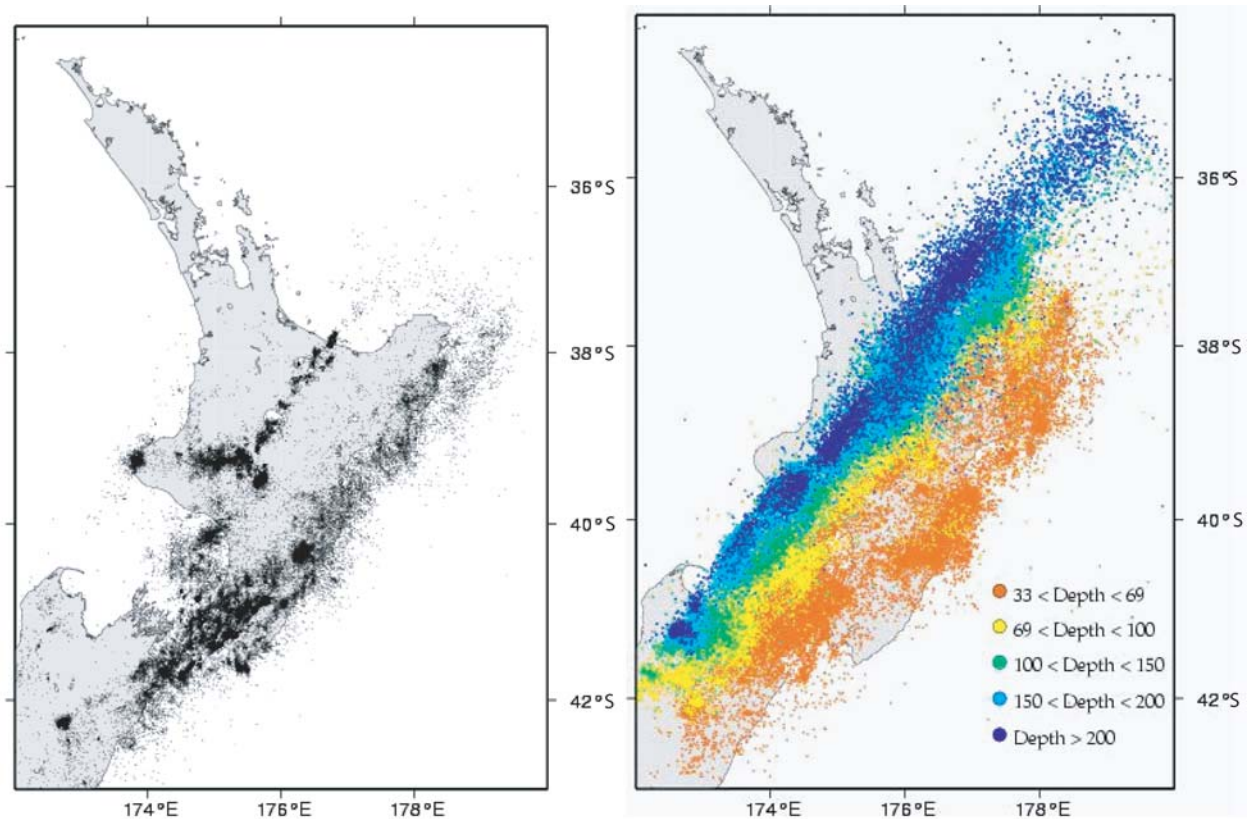
Figure 2. Selected seismicity between January 1990 and December 2007 (inclusive), from the GeoNet database (http://geonet.org.nz). Events shown are only those which were recorded by six or more stations, with nine or more observed phases, with unrestricted location depths, and RMS of arrival time residuals less than 1.0 s. Magnitude range of events shown is 0.29–6.99. (left) Events shallower than 33 km. (right) Events greater than 33-km depth.

able to explain the mechanisms behind seismic behaviour at the Hikurangi margin.

2. Subduction at the Hikurangi Margin

[5] The North Island of New Zealand marks the plate boundary where the 120 Myr old Pacific oceanic lithosphere [*Taylor*, 2006] subducts westward beneath the continental lithosphere of the Australian Plate. The surface expression of the subduction interface occurs along the Hikurangi Trough, offshore the eastern North Island (Figure 1). The subducting slab is well defined by recent seismicity (Figure 2), and seismic tomography studies reveal a high P wave velocity (V_p) region extending to >300 km depth, corresponding to the relatively cold, dense subducting Pacific slab [*Reyners et al.*, 2006].

[6] Within New Zealand, active volcanism related to subduction of the Pacific Plate is largely confined to the central North Island, in the Taupo Volcanic Zone (TVZ) [e.g., *Wilson et al.*, 1995;

Price et al., 2005; *Stern et al.*, 2006], although active volcanism also occurs at Mount Taranaki, well back from the main arc (Figure 1a). Farther north, the Pacific Plate subducts beneath the Kermadec and Tonga arcs, and is associated with shallow and deep seismicity and active arc volcanism. Together, the contiguous Hikurangi, Kermadec, and Tonga trenches constitute a 3000-km-long subduction system (Figure 1c).

[7] Oblique convergence between the Pacific and Australian Plates is partitioned in the North Island [e.g., *Cashman et al.*, 1992; *Beanland and Haines*, 1998; *Webb and Anderson*, 1998]. On geological timescales, most (>80%) of the convergent component of relative plate motion occurs on the subduction thrust, with the remainder accommodated on upper plate reverse faults [*Kelsey et al.*, 1995; *Barnes and Mercier de Lepinay*, 1997; *Barnes et al.*, 1998a; *Nicol and Beavan*, 2003; *Nicol et al.*, 2007; *Nicol and Wallace*, 2007]. The campaign GPS velocity field in the eastern North Island shows that 50–60 mm/yr of convergence
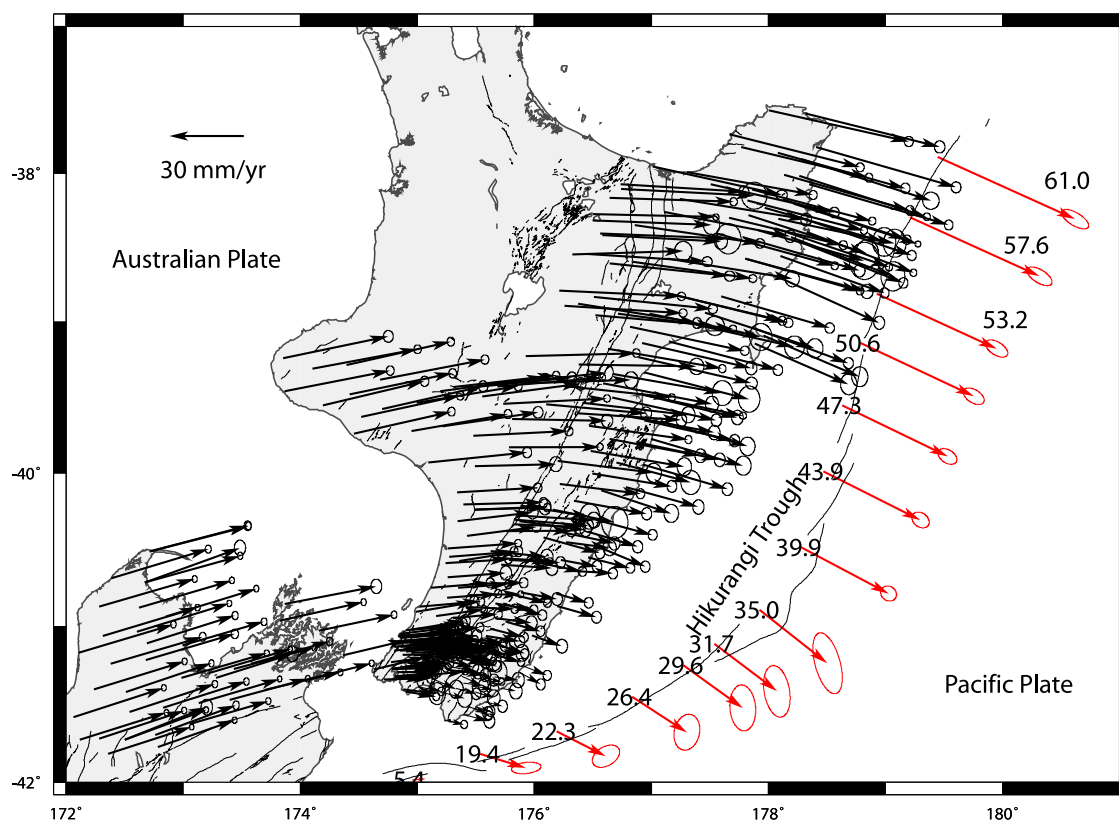
Figure 3. GPS velocities (black) relative to the Pacific Plate. Red vectors show estimated long-term convergence rate at trench labeled in mm/yr [*Wallace et al.*, 2004].

occurs offshore of the northeastern North Island, while these rates decrease to ~20 mm/yr in the southern North Island [*Wallace et al.*, 2004] (Figure 3). This southward decrease in offshore convergence rates is accompanied by an increase in upper plate shortening and produces rapid clockwise tectonic rotation of the eastern North Island relative to the bounding Pacific and Australian Plates [*Walcott*, 1984; *Mumme et al.*, 1989; *Wallace et al.*, 2004]. The margin-parallel component of Pacific/Australia relative plate motion is accommodated by a combination of strike-slip faulting and clockwise rotation of the eastern North Island [*Beanland and Haines*, 1998; *Wallace et al.*, 2004].

[8] Geological mapping combined with offshore seismic reflection and bathymetry studies shows a well-developed imbricated upper plate between the central Hikurangi Trough and the strike-slip faulted axial ranges of the North Island [*Davey et al.*, 1986; *Lewis and Pettinga*, 1993; *Barnes and Mercier de Lepinay*, 1997; *Nicol and Beavan*, 2003]. The frontal wedge is up to 150 km wide, and includes an inner, highly deformed presubduction Cretaceous and Paleogene sequence covered with deformed Miocene-Recent basins, and an outer accretionary wedge of mainly Plio-Pleistocene turbidites [*Lewis and Pettinga*, 1993; *Lewis et al.*, 1998; *Barnes et al.*, 2009] (Figure 4). In the central part of the margin, the accretionary wedge reaches about 70 km in width, and is characterized by long (~100 km) thrust ridges and slope basins [*Davey et al.*, 1986; *Barnes and Mercier de Lepinay*, 1997; *Lewis et al.*, 1998] (Figures 1a and 4b). Seismic reflection data including a variety of archived oil company sections, NIGHT [*Henrys et al.*, 2006], R/V *Sonne* [*Barnes et al.*, 2009], and high-fold data recently acquired by the New Zealand Ministry for Economic Development [*Barker et al.*, 2009], highlight the presence of major thrust faults in the upper plate, many of which splay from the plate interface to the surface. Prominent examples of the latter include the structures beneath the Kidnappers and Lachlan ridges (KR and LR in Figure 1a and also Figure 4b) [*Barnes et al.*, 2002; *Barnes and Nicol*, 2004; *Henrys et al.*, 2006]. From ~41.5°S, the width of the accretionary wedge narrows toward the southwest and fairly dramatically northeastward of Hawke Bay [*Collot et al.*, 1996] (Figure 4). The northern portion of the Hikurangi margin (east of Raukumara Peninsula) is relatively sediment-
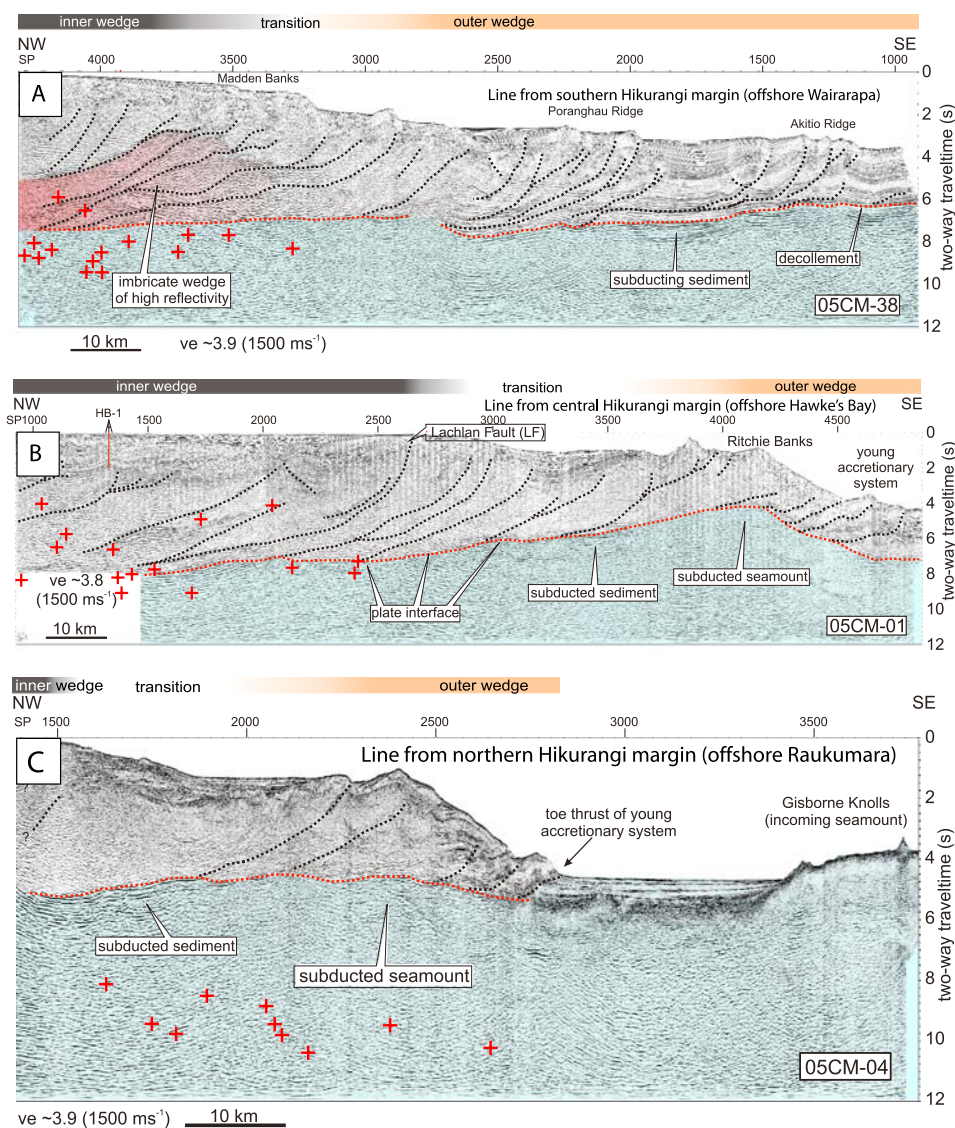
Figure 4. Representative seismic lines from the (a) southern, (b) central, and (c) northern sections of the offshore Hikurangi margin, adapted from *Barker et al.* [2009]. Figure 4a shows seismic reflection line 05CM-38 (location in Figure 1). Dotted red line marks the decollement/plate interface, with shaded blue transparency for subducting material below. The shaded red transparency indicates an imbricate wedge of high-reflectivity material. Red crosses indicates projected positions of earthquakes within 10 km of the section, with depths converted to two-way time using the velocity model discussed by *Barker et al.* [2009]. *Barker et al.* [2009] interpret the transition from inner to outer wedge (bar at the top) to be marked by the break in slope. Numerous splay faults cut the wedge. Young faults toward the toe of the wedge cut a thick section of incoming turbidites, while undeformed sediment can be seen subducting beneath the decollement [see also *Barnes et al.*, 2009]. Figure 4b shows seismic reflection line 05CM-01 (location in Figure 1). Note the splay faults cutting the upper plate, including Lachlan Fault displacing the seafloor. Subduction of a seamount has deformed the outer wedge to produce an outer high (Ritchie Banks), with uplifted slope basins landward and a young, narrow accretionary zone seaward. Figure 4c shows seismic reflection line 05CM-04 (location in Figure 1). As with 05CM-01 this margin has been modified by seamount subduction, with a seamount underlying an outer high. Landward of the high are uplifted slope basins, while seaward is a narrow accretionary zone with an oversteepened slope. Note the incoming seamount, as yet unsubducted, and thin sedimentary cover on the downgoing plate compared with farther south.

starved (Figure 1a) [*Lewis et al.*, 1998], and exhibits frontal subduction erosion associated with subducting seamounts [e.g., *Collot et al.*, 1996, 2001; *Barker et al.*, 2009; R. Bell et al., Seismic reflection character of the Hikurangi subduction interface, New Zealand, in the region of repeated Gisborne slow slip events, submitted to *Geophysical Journal International*, 2009; K. L. Pedley et al., Seafloor structural geomorphic evolution of the accretionary frontal wedge in response to seamount subduction, Poverty Indentation, New Zealand, submitted to *Marine Geology*, 2009] (Figure 4c), and a mix of normal and reverse faulting in the remnant prism.

[9] An important aspect of subduction at the Hikurangi-Kermadec margin is the along-strike variation in the character of the subducting plate. At the Hikurangi Trough, a thick, oceanic plateau (the Hikurangi Plateau) is being subducted; the Pacific plate changes northward to normal oceanic crust (Cretaceous) that subducts at the Kermadec Trench (Figure 1). The Hikurangi Plateau thickens southward from 10 km in the north, to 15 km adjacent to the Chatham Rise [*Davy and Wood*, 1994]. It is studded with seamounts, which are more numerous in the north. The plateau is Cretaceous in age [*Mortimer and Parkinson*, 1996] and covered by a Cretaceous and Cenozoic sedimentary sequence [*Davy et al.*, 2008]. In the Hikurangi Trough, this cover has been inferred to comprise a subducting sequence including >500 m of low velocity ($\sim$2.5–3.5 km/s) Cretaceous volcaniclastics and/or limestone/chert (>100 Myr), $\sim$600 m of Cretaceous clastic sedimentary rocks (100–70 Ma), and $\sim$200 m of Cretaceous-Oligocene pelagic sedimentary rocks (70–32 Ma), and an accreting, upper sequence of mainly Plio-Pleistocene turbidites [*Barnes et al.*, 2009]. The turbidite sequence thickens southward from $\sim$1 km off northeastern North Island to $\sim$6 km off northeastern South Island [*Lewis et al.*, 1998] (Figure 1a). The southward increase in thickness of the subducting Pacific Plate and its cover sequence accompanies a southward decrease in convergence rate at the trench. Subduction terminates where the Chatham Rise (a continental fragment, 27 km thick [*Reyners and Cowan*, 1993]) intersects the margin.

3. Definition of the Hikurangi Subduction Interface Seismogenic Zone

[10] In contrast to the historical occurrence of great subduction interface earthquakes at many of the world's major subduction zones [e.g., *Uyeda and Kanamori*, 1979; *Pacheco et al.*, 1993], no such events have occurred at the Hikurangi margin in historical times (see section 3.3.1). The absence of substantial subduction interface events can be explained in one of two ways: (1) this is a subduction margin where great subduction thrust earthquakes do not occur or (2) great subduction thrust earthquakes do occur here, but the historical record ($\sim$170 years) is simply too short to have captured such events (repeat times for great subduction earthquakes at the Hikurangi margin are probably >300 years; see Appendix B). In either case, we must rely on other types of data (see sections 3.1–3.5) to delineate the likely seismogenic zone of the Hikurangi subduction thrust.

3.1. Geodetic Evidence for Contemporary Interseismic Coupling

[11] The distribution of interseismic coupling on a subduction thrust fault can be estimated from the elastic (recoverable) strain rates transmitted into the crust as measured by surface geodetic (e.g., GPS) networks [e.g., *Savage*, 1983; *McCaffrey et al.*, 2000; *Mazzotti et al.*, 2000; *Norabuena et al.*, 2004]. Locations of contemporary interseismic coupling (see definition of this term in Appendix A) may reveal the likely rupture area of future subduction thrust events. Geodetic data are particularly useful for defining the downdip limit of the interseismically coupled zone (which may correspond to the downdip limit of the seismogenic zone), although they cannot be used to define the updip end [e.g., *McCaffrey*, 2002; *Wang and Dixon*, 2004].

[12] Campaign GPS data have been collected throughout New Zealand since the early 1990s, including at $\sim$300 sites along the Hikurangi subduction margin (Figure 3) [*Beavan and Haines*, 2001; *Darby and Beavan*, 2001; *Wallace et al.*, 2004]. The contractional component of relative plate motion accommodated by faulting in the overlying plate west of the accretionary wedge in the southern North Island is minor, up to $\sim$6 mm/yr [*Walcott*, 1987; *Nicol and Beavan*, 2003; *Nicol et al.*, 2007], and cannot be the sole cause of large contemporary contractional strain rates [*Beavan and Haines*, 2001] observed by GPS in the southern North Island. *Darby and Beavan* [2001] used the GPS data to deduce that the subduction interface beneath the Wellington region is completely interseismically coupled (e.g., $\phi_{ic} \sim 1.0$; see Appendix A) over a 90–110 km wide zone perpendicular to the strike of the margin.
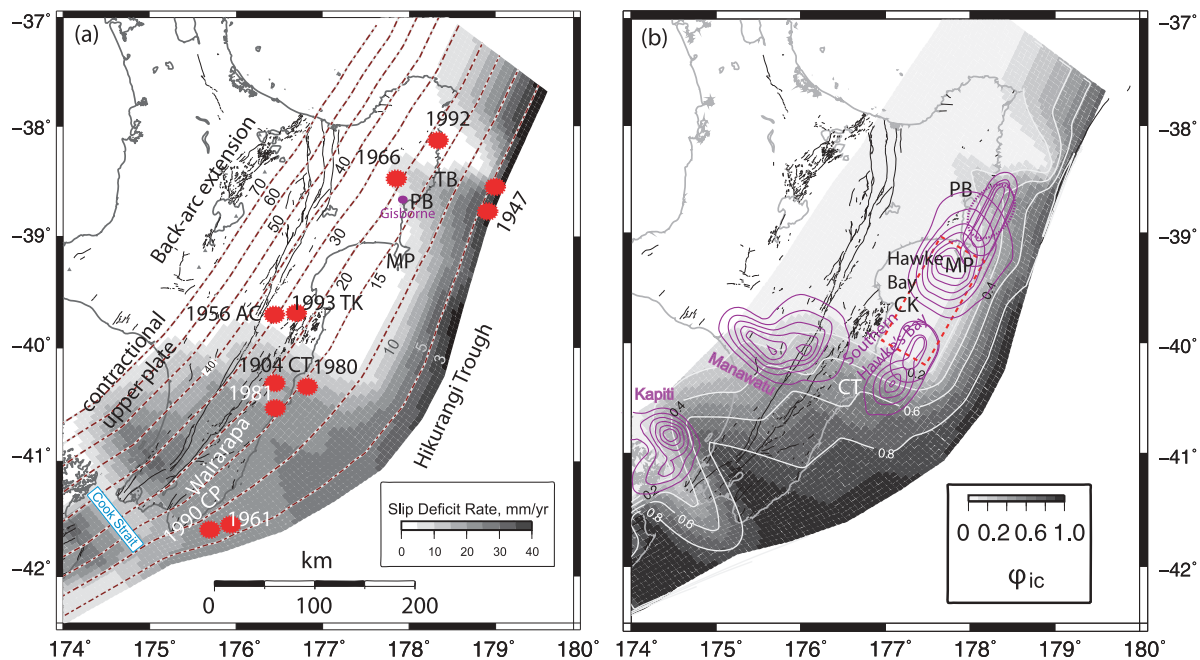
Figure 5. Distribution of interseismic coupling at the Hikurangi margin interpreted from campaign GPS measurements (updated from *Wallace et al.* [2004]). (a) Interseismic slip rate deficit (gray-scale shaded, in mm/yr). Maroon and white dashed lines show contours of model plate interface [from *Ansell and Bannister*, 1996], with depth contours labeled in km. Large red dots show locations of historic subduction interface events from *Webb and Anderson* [1998], *Downes et al.* [2000], and *Downes* [2006]. TK, Tikokino earthquake; AC, Ashley Clinton earthquake; CP, Cape Palliser earthquakes; CT, Cape Turnagain earthquake; TB, Tolaga Bay. (b) Interseismic coupling coefficient, gray-scale shaded and contoured. Locations of slow slip events (purple contours outline areas of slow slip [from *Wallace and Beavan*, 2006; *Beavan et al.*, 2007, 2008; *McCaffrey et al.*, 2008]). Box outlined in red dashes shows region where interseismic coupling estimates from GPS are highly uncertain (because of lack of offshore coverage). GPS can be fit by downdip termination of interseismic coupling within this dashed box, although the exact location of the downdip termination of coupling beneath Hawke Bay cannot be determined from existing data. PB, Poverty Bay; CK, Cape Kidnappers; MP, Mahia Peninsula; CT, Cape Turnagain.

[13] *Wallace et al.* [2004] used GPS velocities and geological fault slip rates to simultaneously invert for the long-term (>1 Myr) tectonic rotation of the eastern North Island [*Walcott*, 1984; *Mumme et al.*, 1989] and the degree of interseismic coupling on the subduction interface along the entire Hikurangi margin. They showed that the GPS-derived interseismic coupling distribution includes a sharp transition from a deep (∼40 km depth) downdip termination of interseismic coupling beneath the southern North Island to a shallow downdip (<15 km) termination of coupling beneath the northern and central parts of the margin (Figure 5). This transition occurs along a line extending from Cape Turnagain (CT in Figure 5a) to the Manawatu region. The coupling coefficient (ϕ_{ic}, see Appendix A) beneath the southern North Island is 0.8−1.0, while $\phi_{ic} = 0.1−0.2$ in the Raukumara Peninsula and Hawke's Bay (i.e., the onland region surrounding Hawke Bay itself) regions. The low ϕ_{ic} observed on

the megathrust in the central and northern Hikurangi margin may be explained by the presence of several small asperities where full interseismic coupling ($\phi_{ic} = 1.0$) occurs (possibly corresponding to subducting seamounts) surrounded by regions of steady aseismic creep ($\phi_{ic} = 0.0$). We note that the degree of coupling beneath Hawke Bay is not well resolved, because of the lack of GPS data in the offshore region (Figure 5b), and that coupling clearly does not extend beneath the land adjacent to Hawke Bay, unlike farther south.

[14] A major (but unproven) assumption underlying our use of interseismic coupling as a proxy for the seismogenic zone is that the portions of the subduction thrust that are currently undergoing coupling will eventually slip in future subduction thrust events, once sufficient stresses have accumulated. This assumption is supported by several examples of subduction interface earthquakes in Japan [*Miura et al.*, 2004; *Ito and Hashimoto*, 2004; *Hashimoto et al.*, 2009] and Sumatra [*Chlieh*

_et al._, 2008], where interseismic coupling estimated from GPS reflects the first-order location of slip in recent great subduction thrust events. Moreover, geodetic measurements in Alaska show that interseismic coupling has now resumed within the source regions of both the 1964 Prince William Sound (M_W 9.2) earthquake [_Ohta et al._, 2006] and the 1986 and 1996 Andreanof earthquakes (both M_W 8) [_Cross and Freymueller_, 2007]. Interseismic coupling also seems to have resumed in the region of the 1995 Antofagasta (M_W 8.1) earthquake [_Chlieh et al._, 2004]. These examples suggest that interseismic coupling can resume relatively quickly following a major subduction thrust rupture (e.g., within years to decades following the event), and that the zone of contemporary coupling often coincides with the rupture zone of major thrust events. However, it is also important to keep in mind that the actual slip distribution in large earthquake rupture is typically heterogeneous, often with a five-fold variation in slip at different locations of the rupture region [e.g., _Subarya et al._, 2006; _Hreinsdóttir et al._, 2006]. Thus, the current interseismic elastic strain accumulation may not reflect subsequent coseismic strain release in detail, and should only be used as rough guide for delineating areas that may be prone to rupture in subduction thrust earthquakes.

3.2. Slow Slip Events at the Hikurangi Margin

[15] In the past decade, time series of nonlinear ground deformations observed by continuous GPS have been interpreted as slow slip events (SSEs) at a number of subduction margins around the world [e.g., _Hirose et al._, 1999; _Dragert et al._, 2001; _Larson et al._, 2004; _Douglas et al._, 2005]. All confirmed subduction zone SSEs observed to date appear to occur in the transition zone between the downdip end of the strongly coupled portion of the subduction interface and the aseismically creeping portion [_Hirose et al._, 1999; _Dragert et al._, 2001; _Obara et al._, 2004]. Moreover, SSEs in southwest Japan and Alaska occur near the downdip rupture limit of historic great subduction thrust earthquakes [e.g., _Ozawa et al._, 2002; _Ohta et al._, 2004, 2006]. Thus, SSEs may help to constrain the location, geometry and spatial extent of the zone of interseismic coupling and the potential maximum extent of subduction interface earthquakes.

[16] Since 2002, more than eight distinct slow slip events in four different locations have been observed along the Hikurangi margin [_Douglas et al._,

2005; _Wallace and Beavan_, 2006; _Beavan et al._, 2007]. In all cases, the locations of SSEs along the Hikurangi margin are revealed to be near the downdip termination of interseismic coupling inferred from GPS data [_Wallace et al._, 2004] (Figure 5).

[17] The 2004–2005 Manawatu SSE (the largest SSE in the North Island to date) is estimated to have involved up to 35 cm of slip on the subduction interface over 1.5 years [_Wallace and Beavan_, 2006] (Figure 5). This event propagated updip along the transition zone from an area of deep coupling beneath the southern North Island to shallower interseismic coupling in the central part of the Hikurangi margin. The Manawatu event released moment equivalent to M_W 7.0. In the Wellington region, offshore of the Kapiti Coast, a probable SSE occurred in 2003 [_Beavan et al._, 2007] and a similar, much better documented event occurred in the Kapiti region during 2008 [_Beavan et al._, 2008] (Figure 5b). Both Kapiti events occurred near the downdip limit of interseismic coupling in the southern North Island.

[18] SSEs in the central and northern Hikurangi margin occur at much shallower depths than the Kapiti and Manawatu events farther south (Figure 5). Modeling of three southern Hawke's Bay events shows that they ruptured adjacent parts of the subduction zone ~20–50 km offshore [_Beavan et al._, 2008; _McCaffrey et al._, 2008], coinciding with the downdip limit of coupling, at 10–15 km depth (Figure 5). Although the slip distributions of the Gisborne SSEs in the Raukumara Peninsula region are less well constrained (Figure 5), the displacements are well fit by slip on the subduction interface close to the shoreline (at ~10–15 km depth), and therefore also consistent with a relatively shallow downdip limit of coupling.

[19] Using triangulation data across the Raukumara Peninsula from 1925 and 1976, and GPS data from 1995, _Arnadóttir et al._ [1999] documented a major change in maximum shear strain rates and the orientation of the azimuth of the principal axis of relative extension in the Raukumara Peninsula from 1925–1976 (when maximum extension was oriented perpendicular to the margin) to the 1976–1995 period (maximum extension was oriented parallel to the margin). GPS campaign data from 1995 to 2004 show a similar orientation of maximum extension and magnitude of shear strain rate to that of the 1976–1995 period, within uncertainty [_Douglas et al._, 2005], suggesting that the present-day regime of interseismic coupling has persisted since at least the mid-1970s. _Arnadóttir et al._

[1999] interpreted the 1925–1976 triangulation data to suggest that a large aseismic slip event had occurred beneath the Raukumara Peninsula sometime during that period; such an event would have been deeper and larger (>2 m of slip) than the episodic slow slip events observed in the Gisborne region with CGPS. We suggest that this temporal change in strain patterns from 1925–1976 may partly be explained by a combination of coseismic slip and postseismic deformation associated with the March and May 1947 subduction thrust earthquakes (M_W 6.9–7.1) offshore Gisborne (see section 3.3.1), in addition to a possible large, slow slip event as suggested by *Arnadóttir et al.* [1999].

[20] Overall, the characteristics of SSEs in the North Island are highly variable, probably reflecting along-strike variability in the depth of interseismic coupling along the Hikurangi margin. SSEs in the Hawke's Bay and Gisborne regions are short (lasting up to a few weeks), and appear to occur frequently (every 1 to 2 years) [*Douglas et al.*, 2005; *Beavan et al.*, 2007]. Much larger SSEs like those seen in the Manawatu and Kapiti regions last longer (1–1.5 years) and probably occur more rarely (perhaps every 5 to 10 years) [*Wallace and Beavan*, 2006].

[21] In Japan and western North America, slow slip events are often spatially and temporally associated with nonvolcanic tremor [*Obara*, 2002; *Rogers and Dragert*, 2003; *Obara et al.*, 2004; *Kao et al.*, 2005]. In careful examination of seismic recordings from the 2004 and 2006 Gisborne slow slip events, and a representative month during the 2004–2005 Manawatu event, no tremor signal has yet been detected in association with Hikurangi SSEs [*Delahaye*, 2008; *Delahaye et al.*, 2009]. However, *Delahaye et al.* [2009] documented reverse-faulting microearthquakes triggered by slow slip events in the Gisborne region. *Delahaye et al.* [2009] suggest that the occurrence of tremor in SSEs may be related to stress drop in the SSE: they point out that SSEs associated with tremor (Cascadia and Nankai Trough) tend to have lower stress drops than SSEs associated with microearthquakes (such as those near Gisborne). *Reyners and Bannister* [2007] suggested that a swarm of earthquakes within the subducted slab near Wellington in 2004/2005 was triggered by stress changes induced by the 2003/2004 Kapiti slow slip event [*Beavan et al.*, 2007]. An M_w 6.6 earthquake in December 2007 located within the subducted slab offshore Gisborne is thought to have triggered a nearby slow slip event that began less than a day

after the earthquake [*François-Holden et al.*, 2008].

3.3. Seismological Data Bearing on Hikurangi Seismogenic Potential

3.3.1. Historical Seismicity on the Subduction Interface

[22] In historical times (post 1840), the Hikurangi plate interface has ruptured during several small to moderate magnitude events, all M_w < 7.2, with the most reliable information coming from the instrumental period from ∼1900 to present (Figure 5a). The largest events identified using post-1917 teleseismic records [e.g., *Webb and Anderson*, 1998; *Doser and Webb*, 2003] occurred in March and May 1947, and were M_W 7.0–7.1 and 6.9–7.1, respectively [*Doser and Webb*, 2003], located 50–60 km east of the coast between Gisborne and Tolaga Bay (TB in Figure 5a) [*Downes et al.*, 2000]. Both have characteristics of "tsunami earthquakes" [*Kanamori*, 1972; *Fukao*, 1979; *Pelayo and Wiens*, 1992; *Tanioka et al.*, 1997] including locations close to the trench where the interface is at very shallow depths, slow rupture velocities (assumed to be ∼1 km/s), long rupture durations (at least 40 and 25 s for the March and May 1947 events, respectively), low energy release at high frequencies resulting in low M_L (5.9; 5.6) compared to M_S (both 7.2) and M_W (7.0–7.1; 6.9–7.1), and larger than expected tsunami (runups of 10 m and 6 m, respectively) [*Downes et al.*, 2000; *Doser and Webb*, 2003]. Other than the 1947 events, the largest known subduction thrust event beneath the northeast part of the margin is the 1966 M_W 5.6 Gisborne earthquake [*Webb and Anderson*, 1998].

[23] In the central part of the margin, from Cape Turnagain to Mahia Peninsula (CT and MP in Figure 5), the largest well-constrained plate interface event is the 1993 M_W 5.6–6.0 Tikokino earthquake (Figure 5a) [*Webb and Anderson*, 1998; *Abercrombie and Benites*, 1998; *Reyners et al.*, 1997a]. The nearby 1958 M_S 5.1 (M_L 6.1 [*Dowrick and Rhoades*, 1998]) Ashley Clinton earthquake, which is notable for the small number of aftershocks, may also have been on the plate interface [*Reyners et al.*, 1997a]. *Downes* [2006] suggested that the 1904 M_W 7–7.2 Cape Turnagain earthquake, located within 80 km of the Tikokino and Ashley Clinton earthquakes (Figure 5a), was on the plate interface.
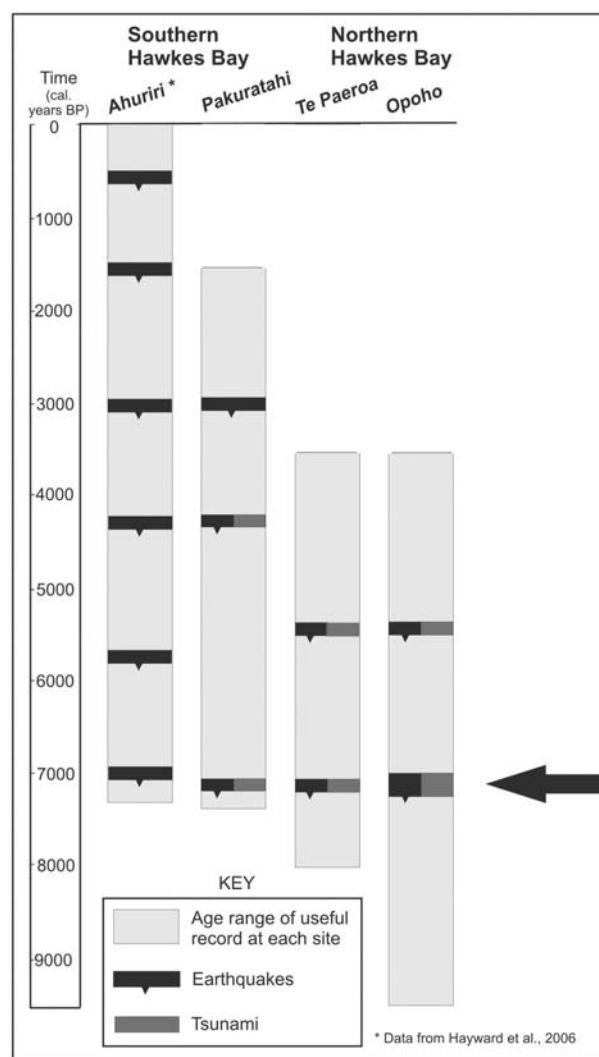
Figure 6. Timeline of subsidence events in Hawke's Bay. Large arrow indicates the time when events correlate between northern (Te Paeroa and Opoho) and southern (Ahuriri and Pakuratahi) Hawke's Bay. Southern Hawke's Bay sites are located near Napier (Figure 8), and northern Hawke's Bay sites are shown in Figure 7. Data from *Cochran et al.* [2006] and *Hayward et al.* [2006].

and *Downes*, 1997; *Little and Rogers*, 2005], could have involved some slip on the deeper (below 25–30 km) subduction interface beneath the lower North Island in conjunction with surface rupture of the Wairarapa Fault [*Darby and Beanland*, 1992; *Beavan and Darby*, 2005]. In summary, most of the historic interplate subduction events have occurred around the periphery of the strongly interseismically coupled part of the subduction interface (for example, the 1904 Cape Turnagain and 1993 Tikokino earthquakes), or in the region of weak interseismic coupling (1947 Gisborne events) (Figure 5a).

3.3.2. Seismological Delineation of the Seismogenic Zone

[25] Because of the lack of great subduction thrust earthquakes at the Hikurangi margin, smaller magnitude earthquake activity has been used to define the seismogenic zone. Moderate magnitude, aftershock deficient events such as the 1993 M_w 5.6–6.0 Tikokino earthquake (Figure 5a) have been interpreted as ruptures of isolated asperities in a region where the plate interface is otherwise in the conditionally stable frictional field [*Reyners et al.*, 1997a; *Abercrombie and Benites*, 1998]. If so, they may indicate regions where ϕ_{ic} is relatively low. This concept can be generalized to all smaller low-angle thrust events near the plate interface; we would not expect such events to occur where ϕ_{ic} is high. Small, low-angle thrust events near the plate interface in Cook Strait and the southernmost North Island concentrate on the edges of the strongly coupled region defined by GPS, with few such events within the strongly coupled region itself [*Reyners et al.*, 1997b]. In contrast, in the Hawke's Bay and Raukumara Peninsula regions, low-angle thrusting events near the plate interface are common [*Reyners and McGinty*, 1999; *Henrys et al.*, 2006], consistent with the inference from GPS that ϕ_{ic} is much lower there. The San Andreas Fault in California may show similar behavior: microseismicity is common on the "creeping" sections of the San Andreas Fault in California [e.g., *Nadeau and McEvilly*, 2004], while there is a distinct lack of seismicity on the segments of the San Andreas that ruptured with large slip in 1906 [*Zoback et al.*, 1999].

3.4. Geological Evidence for Prehistoric Subduction Earthquakes

[26] Uplift and subsidence caused by deformation of the upper plate in subduction earthquakes can be

[24] Along the southern part of the margin (south of Cape Turnagain), portions of the plate interface have ruptured in three, or possibly five, moderate magnitude (M_W 5.4–6.5) earthquakes since 1917 [*Doser and Webb*, 2003]. The two largest events were in 1961 (M_W 6.4–6.5) located about 40 km offshore and in 1990 (M_W 5.6 and M_W 5.5), both to the east of Cape Palliser (CP in Figure 5a). All were near-shore or offshore, indicating that there has been no rupture of the plate interface beneath land since 1917 [*Doser and Webb*, 2003]. The 1855 M_W 8.1–8.4 Wairarapa earthquake [*Grapes*
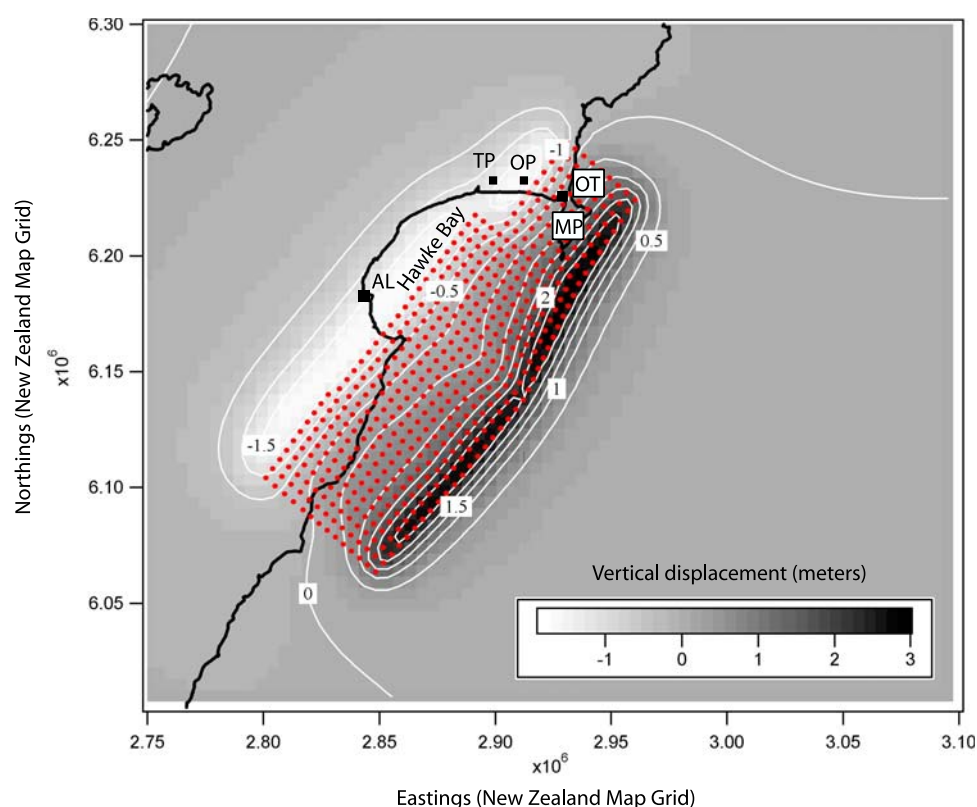
Figure 7. Forward elastic dislocation modeling of subduction interface rupture scenario (8 m slip on subduction interface on patches centered at red nodes) to reproduce 0.5–2 m of coseismic subsidence observed at Te Paeroa (TP) and Opoho (OP) coastal sites in northern Hawke's Bay, with negligible subsidence at Opoutama (OT) and uplift at Mahia Peninsula (MP) [*Cochran et al.*, 2006], and subsidence at Ahuriri Lagoon (AL) in southern Hawke's Bay [*Hayward et al.*, 2006]. Updated from *Cochran et al.* [2006].

recorded in coastal environments as sudden relative sea level changes [e.g., *Atwater*, 1987; *Long and Shennan*, 1994]. Recently, investigation of subsiding parts of the Hawke's Bay region coastline (generally in-board of the uplifted zone, within the fore-arc basin [*Ota et al.*, 1989]) have provided evidence for subsidence and marine submergence events throughout the Holocene (Figure 6) [*Cochran et al.*, 2006; *Hayward et al.*, 2006]. Subsidence events have provided the most robust geological evidence for the occurrence of preinstrumental plate interface earthquakes in other parts of the world [e.g., *Clague*, 1997; *Cisternas et al.*, 2005]. Evidence for sudden subsidence in northern Hawke's Bay includes tsunami deposits overlain by chaotically mixed, reworked sediment that appears to have been deposited rapidly at tidal inlet sites 10 km apart [*Cochran et al.*, 2006] (at Te Paeroa and Opoho; TP and OP in Figure 7). In southern Hawke's Bay, subsidence events at Ahuriri Lagoon (AL in Figure 7) have been identified as sudden decreases in paleoelevation using the tidal elevation preferences of fossil foraminifera [*Hayward et al.*, 2006]. One event (at about 7000 cal yrs BP)

has been correlated between the two sites (∼100 km apart) in northern and southern Hawke's Bay indicating either a single long rupture or two or more ruptures that occurred within decades of each other (Figure 6). This event (or pair of events) also coincides with the formation of two landslide-dammed lakes in central and northern Hawke's Bay [*Howorth and Ross*, 1980; *Page and Trustrum*, 1997]. Elastic dislocation models that fit the subsidence amplitudes imply ∼8 m of slip on the interface that largely occurs offshore, terminating beneath Mahia Peninsula [*Cochran et al.*, 2006] (Figure 7). If we assume that the subsidence events that occurred at ∼7000 cal. years BP in northern and southern Hawke's Bay were indeed synchronous (although the resolution of radiocarbon dating is not good enough to prove this) and occurred on a single structure, then an interface source is likely. Such an event might have affected >100 km of coastline and would have had a magnitude of at least M_W 8.0.

[27] Flights of raised Holocene marine terraces are preserved at numerous coastal localities along the
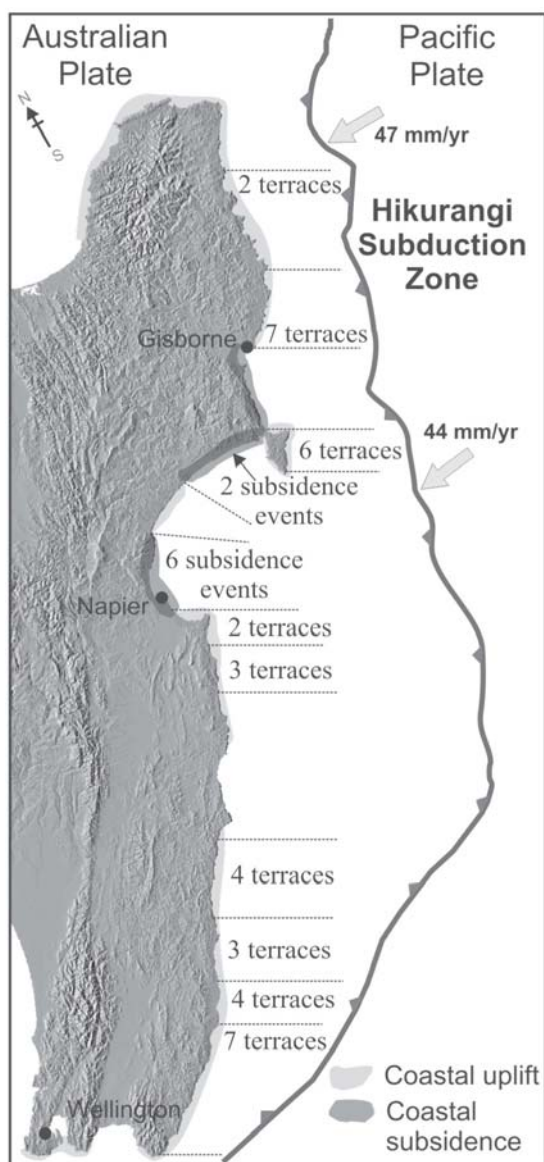
Figure 8. Coastal localities along the Hikurangi Margin exhibiting evidence of coseismic uplift (raised terraces) and coseismic subsidence (drowned water bodies).

Hikurangi Margin (Figure 8). Their stepped morphology and preservation of in situ intertidal fauna are consistent with these surfaces forming via episodic coseismic uplift [e.g., *Hull*, 1987; *Berryman et al.*, 1989; *Ota et al.*, 1990, 1991, 1992; *Berryman*, 1993; *Wilson et al.*, 2006, 2007]. In most cases the tilt inferred to have occurred simultaneously with uplift is too steep to be caused by subduction interface rupture, and these terraces are thus generally inferred to represent deformation caused by movement on local, upper plate faults that splay off the subduction interface [e.g., *Berryman et al.*, 1989; *Ota et al.*, 1991; *Barnes*

et al., 2002; *Wilson et al.*, 2007; *Litchfield et al.*, 2009; F. Paquet et al., Late Pleistocene sedimentation in Hawkes Bay, New Zealand: New insights into forearc basin morphostructural evolution, submitted to *Geological Society of America Bulletin*, 2009] (see Figure 4b). However, it is possible that these upper plate splay faults may sometimes rupture simultaneously with the subduction interface [e.g., *Wang and Hu*, 2006].

[28] Although the complex upper plate tectonics at the Hikurangi margin makes the preservation and interpretation of vertical coastal deformation related to prehistoric subduction interface earthquakes difficult, the subduction interface is the only potentially seismogenic structure at the Hikurangi margin thought to be capable of causing synchronous vertical deformation over long (i.e., >250 km) distances. More detailed dating of coastal coseismic uplift and/or subsidence events and understanding of the effects of upper plate structures are required in order to identify synchronous events at widely spaced locations that may be related to large-scale subduction interface rupture. Away from the coast, preliminary work on uplifted fluvial terraces [*Litchfield*, 2008; *Litchfield et al.*, 2009] and large landslides suggest these features may also provide evidence to help delineate the extent of synchronous widespread vertical deformation.

3.5. Comparison Between GPS, Seismological, and Geological Evidence for the Seismogenic Potential of the Interface

[29] GPS and seismological data indicate that high interseismic coupling occurs beneath the entire southern North Island, over a region 90–180 km wide (across strike), and extending to a maximum depth of ∼40 km (with a possible transition zone to 70 km depth). The southern portion of the Hikurangi margin may thus pose the biggest subduction earthquake hazard to New Zealand, with the potential to rupture in earthquakes on the order of M_W 8.2–8.7 (see Appendix B). There are, however, currently no published paleoseismological investigations specifically targeting evidence for rupture of the strongly coupled portion of the subduction interface beneath the southern North Island, although a few promising sites are currently under investigation.

[30] Interpretation of GPS strain rate measurements, the observation of shallow slow slip events, and the prevalence of shallow thrust earthquakes near the plate interface suggest that interseismic coupling is weaker and shallower in the Hawke's

Bay region compared to the southern Hikurangi margin. The comparatively shallow downdip termination of interseismic coupling just beneath Mahia Peninsula and Cape Kidnappers (MP and CK in Figure 5b), as estimated from GPS, is also consistent with the downdip termination of rupture derived from elastic dislocation modeling of subsidence events that may have been caused by prehistoric subduction interface earthquakes beneath Hawke Bay [*Cochran et al.*, 2006] (Figure 7). However, some seismological studies suggest deeper interseismic coupling beneath the Hawke's Bay region [*Reyners*, 1998, 2000; *Henrys et al.*, 2006]. If the subduction thrust beneath the entire Hawke's Bay region ruptured in a single earthquake, it could be as large as $M_W 8.0-8.3$ (see Appendix B).

[31] Seismological and GPS evidence suggest that interseismic coupling is shallow (<15 km depth) beneath the Raukumara Peninsula, with the exception of a patch of deeper interseismic coupling that extends to 20–25 km depth north of Poverty Bay (PB in Figure 5b). The more frequent occurrence of moderate to large subduction interface earthquakes at the northern Hikurangi margin [*Webb and Anderson*, 1998; *Doser and Webb*, 2003] is consistent with the rupture of small patches of the subduction interface in the portion of the margin where the subduction rate is highest (up to 60 mm/yr; Figure 3). Seamounts being subducted beneath this region [e.g., *Bannister*, 1986; *Collot et al.*, 2001; *Henrys et al.*, 2006; Bell et al., submitted manuscript, 2009] may form isolated asperities (surrounded by velocity strengthening sediment), thus limiting stick-slip behavior to relatively small areas.

4. Physical Controls on Interseismic Coupling and the Geometry of Potential Subduction Interface Ruptures

[32] Whether or not seismogenic rupture can initiate at a particular place on the subduction interface is governed by its shear strength (determined by interface normal stress, pore fluid pressure, stiffness, and the frictional coefficient of the interface material [e.g., *Scholz*, 1990, 1998]). These factors depend on a wide range of parameters that play roles of varying importance for each subduction zone. Such parameters include: subducting sediment thickness, type, and hydrological properties [e.g., *Ruff*, 1989; *Cloos and Shreve*, 1988a, 1988b; *Eberhart-Phillips and Reyners*, 1999], strength/rheology of the upper plate [*McCaffrey*, 1993], temperature [*Tichelaar and Ruff*, 1993; *Hyndman*

et al., 1995, 1997; *McCaffrey*, 1997; *Oleskevich et al.*, 1999]; metamorphic reactions [*Vrolijk*, 1990; *Hyndman et al.*, 1997; *Peacock and Hyndman*, 1999; *Moore and Saffer*, 2001], fluid pressures [*Townend*, 1997; *Moore and Saffer*, 2001; *Saffer*, 2003; *Sibson and Rowland*, 2003; *Fagereng and Ellis*, 2009], the geometry of the subducting plate (i.e., the presence of subducting bedrock highs such as seamounts, ridges or normal-faulted horsts and scarps [*Cloos*, 1992; *Scholz and Small*, 1997; *Mochizuki et al.*, 2008]). Here, we discuss the key factors that may control the potential for subduction interface seismic ruptures at the Hikurangi margin.

4.1. What Processes Might Influence the Configuration of the Seismogenic Zone of the Hikurangi Subduction Thrust?

4.1.1. Thermal Controls

[33] *Hyndman et al.* [1997] argue that the downdip limit of the seismogenic zone is largely determined by the intersection between the subduction thrust interface and the 350°C isotherm or the fore-arc Moho, whichever is shallower. The transition from velocity-weakening to velocity-strengthening behavior in some tested rocks, and from brittle to viscous deformation modes in quartz dominated lithologies, both occur at ~300–350°C [e.g., *Sibson*, 1984; *Tse and Rice*, 1986; *Blanpied et al.*, 1991]. Stable sliding should occur on faults where these temperatures are exceeded, providing a downdip limit for seismogenesis, although some transitional stick-slip/stable-sliding behavior may occur down to 450°C [e.g., *Hyndman and Wang*, 1993; *Tichelaar and Ruff*, 1993]. Thermal models of subduction interfaces at the Cascadia margin, southwest Japan (Nankai), Mexico, and South America have been used to explain the downdip termination of the seismogenic zone to a first order [*Hyndman et al.*, 1997; *Oleskevich et al.*, 1999; *Currie et al.*, 2002].

[34] The downdip transition from interseismic coupling to aseismic creep in the southern Hikurangi margin occurs where temperatures are estimated to be between 300 and 400°C (Figure 9) [*McCaffrey et al.*, 2008; *Fagereng and Ellis*, 2009], suggesting a possible thermal control on the position of the geodetically inferred transition zone in the southern Hikurangi margin. However if the downdip limit of interseismic coupling in the central and northern Hikurangi margin were also controlled by the depth of the 350°C isotherm, it should be much
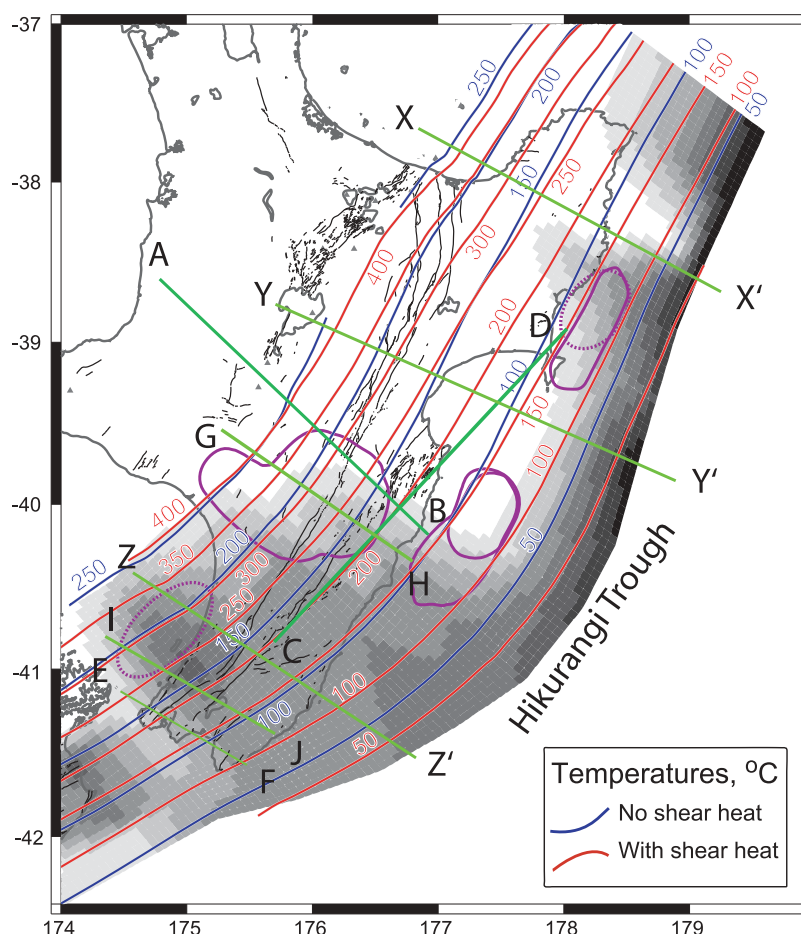
Figure 9. Calculated temperature contours for the subduction interface (in °C) from thermal modeling of heat flow data [*McCaffrey et al.*, 2008]. Temperatures are superimposed on geodetic coupling estimates and slow slip events (see also Figure 5). Blue curves are temperatures with no shear heating included; red curves show temperatures that include shear heating from 20 MPa of stress at all depths. Adapted from *McCaffrey et al.* [2008]. Thick green lines show locations of seismic tomography cross sections in Figure 10 (E–F), Figure 12 (G–H and I–J), and Figure 13 (A–B and C–D); X–X′, Y–Y′, and Z–Z′ show locations of schematic cross sections in Figure 14.

deeper, at ∼35−60 km depth rather than at 10−15 km depth as currently deduced from interseismic coupling estimates and the location of slow slip events (Figure 9) [*McCaffrey et al.*, 2008; *Fagereng and Ellis*, 2009]. Thus, temperature alone cannot explain our observations of a major along-strike variation of the depth of interseismic coupling and location of slow slip events.

4.1.2. Intersection of the Fore-Arc Moho With the Subduction Interface

[35] The intersection between the subducting plate and the serpentinized fore-arc Moho could also provide a lower depth limit for seismogenesis, as serpentinites are thought to be stable-sliding [e.g., *Ruff and Tichelaar*, 1996; *Hyndman et al.*, 1997; *Peacock and Hyndman*, 1999]. The Moho/interface intersection is at ∼40 km depth beneath the southern North Island [*Stern and Davey*, 1990], similar to the downdip limit of interseismic coupling. Qp tomography beneath the southern North Island ("Q" is the quality factor of seismic waves, and is inversely related to attenuation; Qp refers to P waves, and Qs is the quality factor of S waves) shows a small reduction in Qp at about this depth [*Eberhart-Phillips et al.*, 2005] (see Figure 10), suggesting that serpentinization of the mantle wedge might explain the onset of aseismic subduction interface creep in this region. However, the intersection of the fore-arc Moho with the subduction interface cannot explain the inferred shallow (∼10−15 km) downdip transition to aseismic creep in the central and northern portion of the Hikurangi margin, where crustal thicknesses are similar to
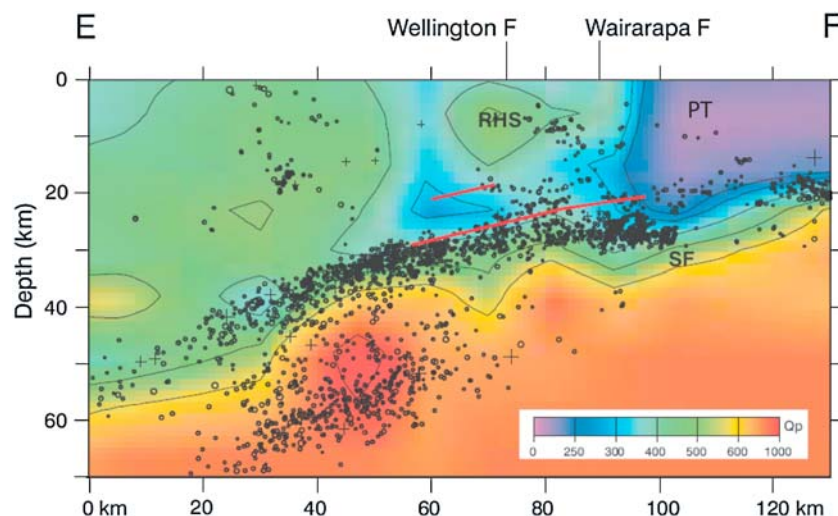
Figure 10. A depth section normal to the strike of the subducted plate in the southern North Island (line E–F in Figure 9) of Qp. Pluses are earthquakes near the section used in the inversion, and circles are double-difference relocations of earthquakes during the period 1990–2001. SF denotes the seismic front for small earthquakes in the top of the subducted plate. Its location appears to be related to the change in terranes in the overlying plate from the low Qp in the Pahau terrane (PT) to the higher Qp Rakaia/Haast Schist terrane (RHS). The major dextral surface faults, the Wairarapa and Wellington faults, are shown. Red lines show seismic reflectors [*Davey and Smith*, 1983]. Drafted using data from *Eberhart-Phillips et al.* [2005].

that found in the southern North Island (e.g., 35–40 km), with the exception of the northern half of the Raukumara Peninsula where upper plate crustal thickness decreases to ~18 km [*Reyners et al.*, 1999].

4.1.3. Upper Plate Structure

[36] The three-dimensional distribution of rock types surrounding the plate interface could play an important role in controlling plate coupling. Recent detailed geologic mapping [*Mortimer*, 2004] and 3-D tomographic inversions for Vp, Vp/Vs and Qp throughout the Hikurangi subduction zone using local earthquakes [*Eberhart-Phillips and Reyners*, 1997; *Eberhart-Phillips and Chadwick*, 2002; *Eberhart-Phillips et al.*, 2005, 2008; *Reyners et al.*, 1999, 2006], and ambient noise Rayleigh wave tomography [*Lin et al.*, 2007] allow us to investigate the influence of rock type. In the crust, increased porosity, crack density, and fluid volume can all decrease Vp and increase attenuation (i.e., reduce Qp) [e.g., *Winkler and Murphy*, 1994]. High fluid volume can also contribute to a higher Vp/Vs [*Eberhart-Phillips et al.*, 1989]. On the basis of their interpretation of the tomography results, *Eberhart-Phillips et al.* [2005] and *Reyners and Eberhart-Phillips* [2009] suggest that the rheology of the lower crust of the overlying plate is a factor in large-scale plate coupling, with the strong coupling in the southern North Island

due to the competent Rakaia/Haast Schist terrane being in contact with the plate interface in this region. They also suggest that the Rakaia/Haast Schist terrane acts as an aquiclude for fluids at the interface, consistent with the observation of a seis-
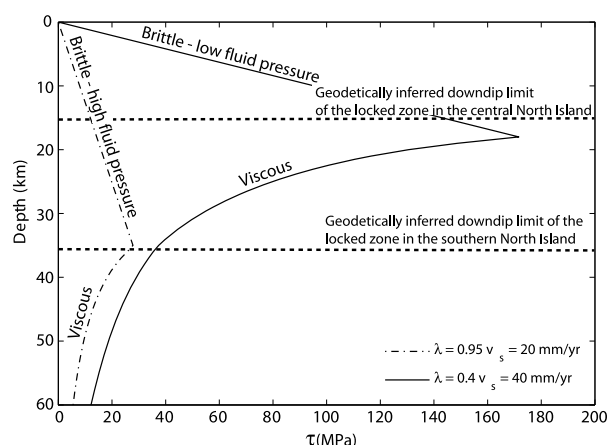

Figure 11. Interface shear strength based on calculated thermal structure from *Fagereng and Ellis* [2009]. Note two distinct depths for the theoretical brittle-viscous transition, a shallow (18 km) transition related to hydrostatic fluid pressure within the upper plate and a deep (35–40 km) transition if the upper plate and interface are near-lithostatically overpressured. For comparison the inferred depths of the locked zone below Hawke Bay and Wellington are also shown. λ = pore fluid factor (P_f/σ_n, where P_f = pore fluid pressure and σ_n = normal stress on the fault plate); V_S = convergence velocity. Adapted from *Fagereng and Ellis* [2009].
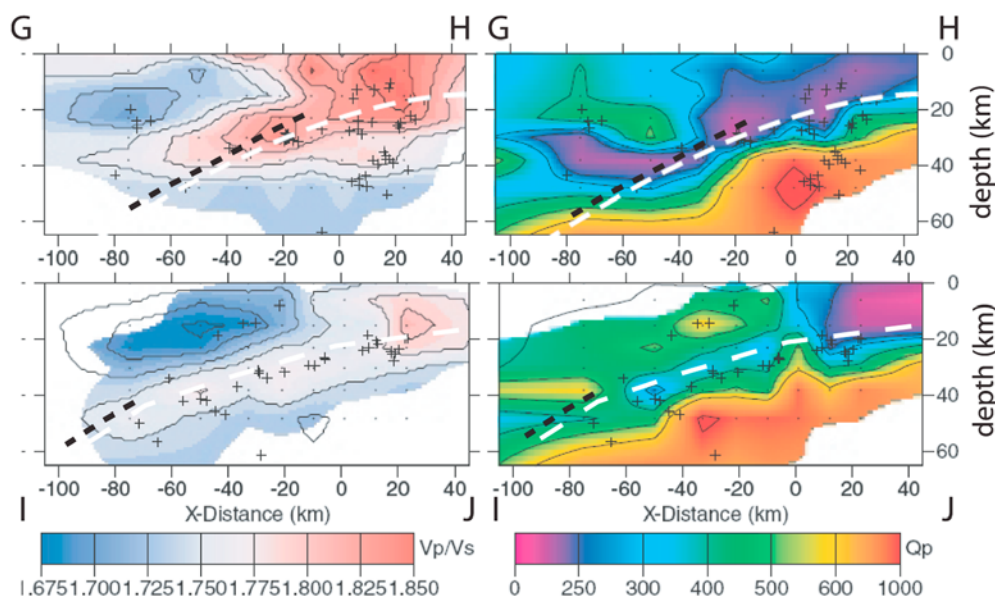
Figure 12. (top) High Vp/Vs and low Qp near the plate interface in a weakly coupled portion of the Hikurangi margin and (bottom) the same but for a strongly coupled region. Lower Vp/Vs and higher Qp occur near the plate interface in the region of strong coupling (cross section I–J across southern part of the margin). Approximate locations of Manawatu slow slip event along section G–H and the Kapiti slow slip event along section I–J shown with heavy black dashed lines. Dashed white line is approximate location of the plate interface. Section locations shown in Figure 9. Data from *Eberhart-Phillips et al.* [2005].

mic reflector at the plate interface underlying the Rakaia/Haast Schist terrane that could indicate the presence of fluids there [*Davey and Smith*, 1983].

4.1.4. Role of Fluid Pressures at the Subduction Margin

[37] Fluids clearly play an important, but complex role in the state of stress and frictional stability on the subduction megathrust. For example, excess fluid pressures reduce the effective normal stresses on the interface, leading to lower frictional shear resistance to slip, and also has an uncertain effect on slip stability [*Scholz*, 1998; *Liu and Rice*, 2007]. On the other hand, *Fagereng and Ellis* [2009] show that for a viscoplastic medium the theoretical brittle-viscous transition is much shallower if the upper plate is in a hydrostatically fluid pressured regime than for a lithostatically pressured regime (Figure 11). Their observations suggest that high fluid pressures within the upper plate and on the interface may favor the occurrence of stick-slip behavior to greater depths than for regions of lower fluid pressures.

4.1.4.1. Subducting Sediments and Associated Elevated Fluid Pressures

[38] If subducted sediments are present, excess fluid pressures can develop within them, which reduces the effective normal stress on the interface,

and could lead to lower frictional shear resistance to slip. This is particularly so where subducting sediments are dominated by fine-grained pelagic clays with poor drainage characteristics [*Townend*, 1997; *Sibson and Rowland*, 2003]. Modeling of Sp converted phases by *Eberhart-Phillips and Reyners* [1999] indicate a 1–2 km thick low-velocity zone (Vp = 5.0–5.3 km/s, Vp/Vs = 2) at the plate interface beneath the Raukumara Peninsula, which they interpret as a channel of fluid-rich sediment. North of Tolaga Bay (TB in Figure 5), they suggest this channel may locally be as thick as 5 km. Similarly, marine seismic reflection profiles east of Gisborne image a subducting sediment channel, beneath the middle to upper slope at least 1 km thick [*Barker et al.*, 2009; Bell et al., submitted manuscript, 2009]. Landward of an inferred subducted seamount, a wedge of subducted sediments 2–4 km thick constitutes a highly reflective zone adjacent to the subduction interface, and coincides with the source region of the 2004 Gisborne slow slip event (Bell et al., submitted manuscript, 2009).

[39] We see evidence of changes in physical properties near the plate interface along strike coinciding with the changes in depth of interseismic coupling, which may be associated with spatial variations in the thickness of subducted and/or underplated sediment (i.e., subducting sediments accreted to the base of the upper plate) and/or
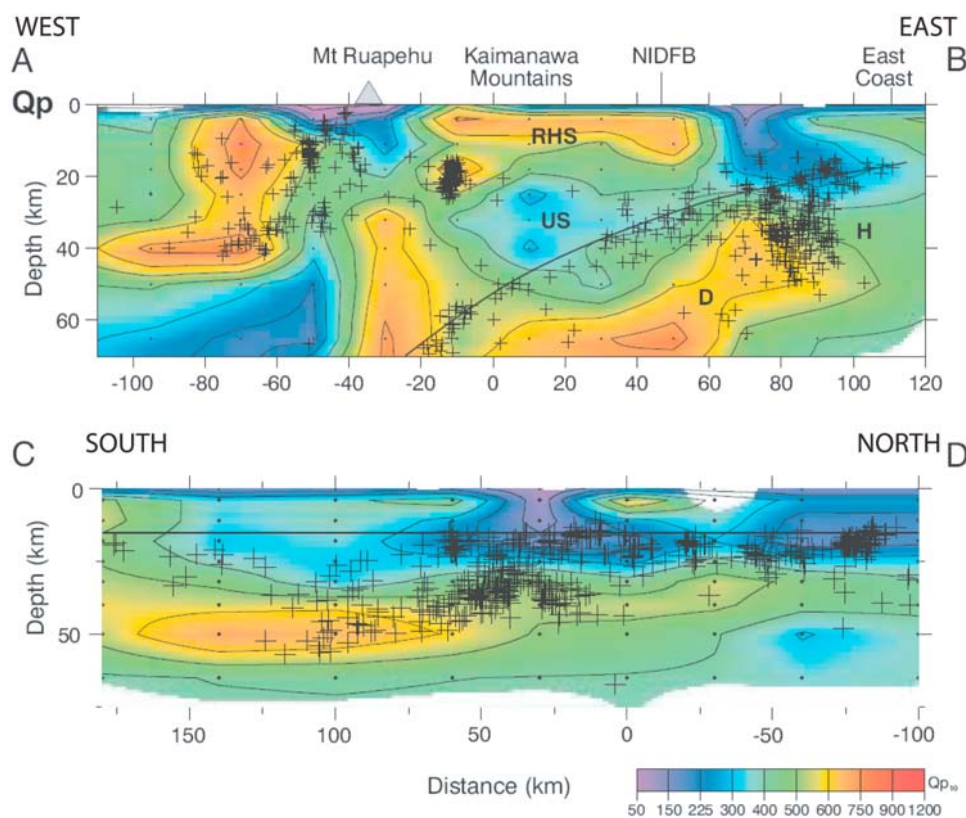
Figure 13. Depth sections normal to strike (line A–B in Figure 9) and along strike (line C–D in Figure 9) of the subducted plate in the central North Island of Qp. The approximate location of the plate interface is denoted by the solid line, and pluses are earthquakes near the section. In the subducted plate, H denotes hydrated regions, and D denotes relatively more dehydrated regions, with the intervening seismicity interpreted as resulting from dehydration embrittlement. In the overlying plate, *Eberhart-Phillips et al.* [2008] interpret RHS as the Rakaia/Haast Schist terrane and US as underplated sediment. NIDFB denotes the North Island dextral fault belt. Qp data are from the inversion of *Eberhart-Phillips et al.* [2008].

abundant fluids (Figures 12 and 13) [*Eberhart-Phillips et al.*, 2005]. In southern Hawke's Bay where interseismic coupling is relatively weak, Vp/Vs is high and Qp is low near the plate interface down to about 40 km depth (Figure 12, section G–H), consistent with the presence of a significant amount of fluid-rich subducted and/or underplated sediment. Despite these observations, we must point out that the inferred presence of fluids from the tomography results does not necessarily indicate suprahydrostatic overpressures, particularly if porosity is high [cf. *Mitsui and Hirahara*, 2008]. Farther southwestward along strike (in the strongly coupled region), Vp/Vs is much lower and Qp much higher above the plate interface, suggesting less low-velocity, underplated sediment there and/or less abundant fluids than farther to the north. In short, the seismic tomography results can be interpreted as revealing a change from extensive sediment subduction/underplating (central and northern North Island) to an accretionary wedge-dominated system (Figure 4a) with a smaller amount of

sediment subduction and/or underplating (southern North Island) (Figure 1). However, subducted sediment has been imaged near the interface from seismic reflection data at the southern Hikurangi margin (Figure 4a). Thus, it is unclear whether the amount of subducted sediment actually does change significantly along the margin, making it difficult to call upon sediment subduction variations as the sole explanation for the along-strike variations in coupling that we see at the Hikurangi margin.

4.1.4.2. Influence of Fluid Pressure State on the Depth to the Brittle/Viscous Transition

[40] *Fagereng and Ellis* [2009] suggest that fluid pressures in the overlying plate and at the subduction interface can influence the depth to the brittle-viscous transition for the Hikurangi margin. For example, their modeling suggests that the brittle/viscous transition occurs at ∼35 km depth (similar to the southern North Island) if the upper plate and

interface have near lithostatic pore pressure, while hydrostatic fluid pressures in the upper plate cause the brittle/viscous transition to occur at much shallower depths (∼18 km; Figure 11), similar to the downdip limit of coupling inferred in the Raukumara and Hawke's Bay regions.

[41] The interpretation of seismic tomography results that the fore arc and interface at the central and northern portion of the Hikurangi margin are fluid-rich, as described above, apparently contradicts the suggestion of *Fagereng and Ellis* [2009] that low (near hydrostatic) fluid pressure conditions prevail there. However, high fluid volumes do not necessarily indicate near-lithostatic fluid pressures, unless the porosity of the surrounding rock is also low. So, if displacement occurs by hydrofracturing, small earthquakes or recurring slow slip events (as we observe at the northern and central Hikurangi margin), fluids can be remobilized by increased structural permeability, and are therefore not isolated, and overpressure is not contained [*Behrmann*, 1991; *Fagereng and Ellis*, 2009]. Geochemical evidence supports the idea of greater fluid mobilization and higher permeability in the northern and central part of the margin versus the southern margin. ^{3}He/^{4}He ratios from hot springs and mud volcano-type springs along the eastern North Island suggest that fluids emerging at the surface in the northern and central Hikurangi margin contain a signature consistent with the mantle of the subducted plate, whereas fluids emitted from springs at the southern portion of the margin have little or no mantle component [*Giggenbach et al.*, 1993]. This observation is consistent with the suggestion of *Reyners and Eberhart-Phillips* [2009] that plate coupling is influenced by the ability of fluid to cross the plate interface.

[42] Unfortunately, there are too few direct measurements of fluid pressures within the upper plate of the Hikurangi margin to test whether or not there is a major decrease in fore-arc fluid pressures from south to north. Those data that do exist (from shallow oil exploration boreholes) suggest fluid pressures close to lithostatic in most locations along the Hikurangi margin [e.g., *Allis et al.*, 1998; *Sibson and Rowland*, 2003], rather than a change to hydrostatic conditions farther north. Accretionary wedge geometry may provide some insight into the fluid pressures along the Hikurangi margin [*Davis et al.*, 1983]. South of Hawke Bay, the accretionary wedge taper is smallest (4−5° [*Barker et al.*, 2009; *Barnes et al.*, 2009]). In the central (Hawke's Bay) portion of the margin,

wedge taper steepens (taper angle is 6−7°), while the largest wedge taper occurs offshore the Raukumara peninsula region (∼10°) (taper angles calculated using data derived from *Barker et al.* [2009]) (Figure 4). Generally, this wedge geometry supports the presence of elevated pore pressures and retarded fluid escape in the southern portion of the Hikurangi margin (low effective stress interface), and low pore pressure, and rapid fluid escape in the northern and central part of the margin (where the Fagereng and Ellis model postulates a high effective stress interface) [cf. *Saffer and Bekins*, 2006]. *McCaffrey et al.* [2008] suggest that high shear stress on the subduction interface is unlikely anywhere along the Hikurangi margin because of the lack of evidence for high surface heat flow that would indicate shear heating. However, *Fagereng and Ellis* [2009] were able to fit low surface heat flow values successfully using a model with high shear stress on the shallow portion (<18 km depth) of the subduction interface. It is unclear why there is a discrepancy between the results of *McCaffrey et al.* [2008] and *Fagereng and Ellis* [2009] regarding the effect of shear heating on the surface heat flow, although it may be due to the different approaches used by the two studies: *McCaffrey et al.* [2008] uses a one-dimensional analytical approach, and assume a linear geotherm, while *Fagereng and Ellis* [2009] use a two-dimensional finite difference approach, and incorporate a more realistic geotherm that accounts for the two-dimensional cooling effect of the slab.

4.1.5. Subducting Plate Structure

[43] Subducting seamounts and other irregularities on the subducting plate may also influence the geometry of the seismogenic zone [e.g., *Cloos*, 1992; *Scholz and Small*, 1997; *Tanioka et al.*, 1997; *Bangs et al.*, 2006], although whether subducted seamounts increase or reduce interseismic coupling is still under debate [e.g., *Mochizuki et al.*, 2008]. The seismogenic character of the northern and central Hikurangi megathrust may be influenced by the presence of subducting seamounts (which are abundant there) surrounded by subducted sediments (Figures 4b and 4c). Historically, subduction interface seismicity in this region is characterized by shallow (<20 km), M_w < 7.1 events. Some of these earthquakes are characterized as "slow" ruptures [*Downes et al.*, 2000], consistent with rupture propagation into surrounding low-rigidity sediments in the conditionally stable field [e.g., *Okal*, 1988]. Using offshore seismic reflection data, Bell et al. (submitted man-
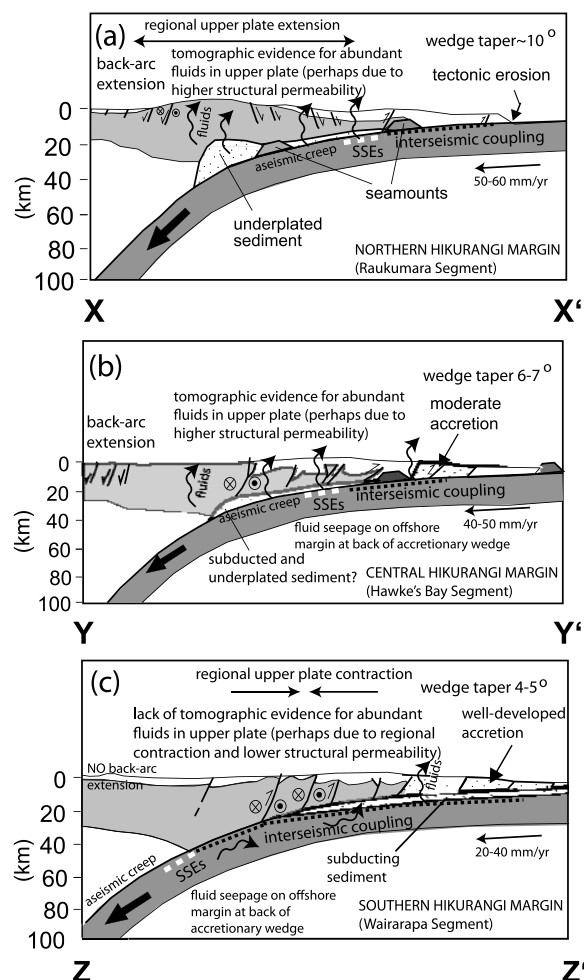
Figure 14. Schematic cross sections summarizing the major processes occurring in the (a) northern, (b) central, and (c) southern portions of the Hikurangi margin. Locations of cross sections given in Figure 9. White dashed line near interface shows approximate location of slow slip events (SSEs), and black dashed line shows approximate location of zone of interseismic coupling.

uscript, 2009) identify a seamount being subducted in the source area of the March 1947 subduction interface earthquake, suggesting that this seamount acted as an asperity for the earthquake. In contrast, the classical form of the accretionary wedge adjacent to the southern Hikurangi margin (Figure 4a) suggests that substantial relief has not been subducted there for at least several million years [*Barnes et al.*, 2009].

[44] Significant changes in slab dip coincide with the downdip limit of interseismic coupling. *Barker et al.* [2009] map the shallow interface geometry to depths of ∼20 km from seismic reflection data along the margin 200 km north and 200 km south of Hawke Bay. They observe that south of Hawke Bay the interface is relatively smooth and dips at

less than 8°, whereas in Hawke Bay and to the north, a distinct kink in the interface is apparent, with a downdip increase in dip to angles greater than 8° at depths of 10–15 km [see also *Henrys et al.*, 2006]. The depth at which the interface steepens is similar to the location of slow slip events beneath this portion of the margin. *Barker et al.* [2009] suggest that this kink may have a profound effect on interface seismogenic properties.

4.1.6. Along-Strike Change From Tectonic Contraction to Extension

[45] North Island deformation undergoes a change from tectonic contraction in the south and east to back-arc extension in central North Island (Taupo Rift, in the Taupo Volcanic Zone (Figure 1) [*Beanland and Haines*, 1998; *Wallace et al.*, 2004; *Nicol et al.*, 2007]). The region of very strong interseismic coupling is below the contractional portion of the upper plate, while the regions of weaker interseismic coupling are adjacent to the region of back-arc rifting in the upper plate (Figure 5a). Although there is some faulting related to upper plate contraction in the region of weak interseismic coupling, this is largely restricted to the offshore accretionary wedge with few active reverse faulting structures at the central and northern Hikurangi margin occurring >30 km inland from the east coast (http://maps.gns.cri.nz/website/af/). Maximum extensional stress orientations in the Raukumara Peninsula crust (estimated from earthquakes in the upper plate) are perpendicular to the trench [*Reyners and McGinty*, 1999], and there are mapped normal faults just to the west of Mahia Peninsula (MP, Figure 1) and throughout the Raukumara Peninsula (Figure 1) (http://maps.gns.cri.nz/website/af/). This is in contrast to the southern North Island where faulting related to recent contractional deformation is common all across the region [e.g., *Lamarche et al.*, 2005; *Nicol et al.*, 2007]. Previous workers have noted a correlation between subduction zones with weak seismic coupling coefficients and an extensional upper plate [e.g., *Scholz and Campos*, 1995], although the mechanism, if any, causing this correlation to occur is currently unclear.

4.2. Our View: Seismogenic Zone Geometry Is Influenced by Multiple Parameters

[46] A number of phenomena occurring at the Hikurangi margin clearly influence the frictional properties and stress at the subduction interface,

and the future likelihood of large subduction thrust earthquakes (Figure 14). A key observation to explain is the unusually abrupt along-strike change in depth to the downdip limit of interseismic coupling and depth, duration, and size of slow slip events that we observe (Figure 5). These changes are likely due to interactions and feedbacks between some or all of the aforementioned processes, and perhaps additional processes that we have not yet considered, such as fault dilatancy stabilization [Segall and Rice, 1995; Rubin, 2008].

[47] The upper plate in the southern North Island undergoes long-term tectonic contraction, and the Rakaia/Haast Schist terrane (which may behave as an impermeable aquiclude [Eberhart-Phillips et al., 2005]) is in contact with the seismogenic portion of the subduction interface beneath the southern North Island. Because of the overall contractional stress regime, and the presence of a somewhat impermeable terrane, near-lithostatic pore pressure conditions probably occur within the upper plate and on the subduction interface beneath the southern North Island. The depth to the brittle/ductile transition in the lower North Island is expected to occur at ~35 km depth where temperature is near ~350°C [McCaffrey et al., 2008], assuming fluid pressures in the upper plate are near lithostatic [Fagereng and Ellis, 2009]. This depth is also comparable to the depth to the fore-arc Moho, suggesting that either the brittle/ductile transition at 350°C, or the depth to the fore-arc Moho provides a downdip limit to the deep interseismic coupling beneath the southern North Island. Thus, upper plate structure, thermal conditions, regional tectonic stress regime, depth to the fore-arc Moho, and fluid pressures may all play a role in producing the deep interseismic coupling we observe there.

[48] The onshore portion of the fore arc at the northern Hikurangi margin is experiencing a mildly extensional tectonic stress regime, while both the central and northern portions of the margin are adjacent to back-arc rifting in the TVZ. Structural permeability of the overlying plate in the north and central Hikurangi margin may be enhanced, as hydrofracturing, and consequent movement of fluids though fractures, is more readily achieved in an extensional stress regime [e.g., Behrmann, 1991; Sibson and Rowland, 2003]. Moreover, hydrofractures in an extensional tectonic regime will be oriented vertically, thus promoting structural permeability (in a contractional regime, hydrofractures are subhorizontal, and do not enhance

permeability [e.g., Sibson, 1992]). Although interpretation of seismic tomography results suggest abundant fluids within the upper plate and surrounding the interface at the Raukumara and Hawke's Bay segments of the margin, the porosity of the upper plate may be so high that fluid pressure (P_f) conditions can still remain close to hydrostatic, thus promoting a shallow brittle-viscous transition (~18 km) [Fagereng and Ellis, 2009]. Another mechanism that may play a role in producing the shallow coupling we observe in the northern and central Hikurangi margin is fault dilatancy stabilization [Segall and Rice, 1995; Rubin, 2008], which could strongly influence the depth to the downdip limit of interseismic coupling [Liu et al., 2008]. In the Raukumara and Hawke's Bay region, subducting seamounts may act as asperities that rupture in subduction thrust earthquakes, similar to the March and May 1947 tsunami earthquakes offshore Gisborne. Subducted and underplated sediment will also influence the frictional properties of the interface locally. Thus, lower plate structure, adjacency to an extensional tectonic stress regime, sediment subduction, and P_f conditions all play a role in the distribution of interseismic coupling that we observe in the Raukumara and Hawke Bay segments.

[49] The sharp change from deep interseismic coupling in the south, to shallow interseismic coupling farther north is mirrored by the abrupt northward change to low Qp and high Vp/Vs of material in the upper plate and near the subduction interface, which may indicate a larger volume of fluids within the northern and central Hikurangi margin (Figures 12 and 13) [Eberhart-Phillips et al., 2005, 2008]. Both of these changes also occur at the same latitude as the southern termination of back-arc extension in the central North Island (south of this point, upper plate tectonics is dominated by contraction; Figure 5a). One way to explain this correlation is that where the upper plate is mildly extensional, and vertically oriented hydrofractures are common, structural permeability will be promoted and fluids will be able to migrate easily throughout the upper plate. Enhanced structural permeability in the north could cause near-hydrostatic P_f to occur, relative to farther south (where P_f may be close to lithostatic); this change in upper plate P_f could lead to a major along-strike change in the depth to the brittle/viscous transition and the downdip limit of coupling that we observe on the subduction thrust [cf. Fagereng and Ellis, 2009].

[50] Our proposed explanation for the transition from deep to shallow coupling at the Hikurangi

margin is largely based on theoretical studies and is mainly untested. Clearly, there are conflicting lines of evidence for and against the existence of higher structural permeability and lower P_f within the fore arc, and higher stresses on the interface in the northern and central portion of the margin (relative to the south), as required by the *Fagereng and Ellis* [2009] model. Those data favoring low P_f and a high-stress interface in the Raukumara and Hawke's Bay regions include (1) an increased accretionary wedge taper angle in the northern and central part of the margin (relative to farther south [cf. *Barker et al.*, 2009]); (2) geochemical evidence for free flow of fluids from the mantle of the Pacific Plate to the surface in the northern and central margin, while fluids from seeps and hot springs in the south do not show a mantle component [*Giggenbach et al.*, 1993]; and (3) tomographic evidence for abundant fluids within the fore arc of the central and northern Hikurangi margin (with a lack of evidence for substantial fluids within the southern fore arc) [*Eberhart-Phillips et al.*, 2005], which we suggest can be attributed to higher structural permeability of the northern and central fore arc. Conversely, data from the few shallow exploration boreholes in the northern and central Hikurangi fore arc suggest near-lithostatic P_f [*Allis et al.*, 1998; *Sibson and Rowland*, 2003], casting some doubt on the assertion that the upper plate in the northern and central Hikurangi margin has near hydrostatic P_f. More data regarding P_f conditions and the porosity/permeability of the North Island crust, studies of existing seeps and springs that occur all along the Hikurangi margin [e.g., *Henrys et al.*, 2009; *Barnes et al.*, 2009], and improved heat flow data are all required to test these ideas.

4.3. Similarities Between Processes at the Hikurangi Margin and Other Subduction Margins

[51] Striking similarities between the Hikurangi subduction margin and other margins are clear. In southwest Japan at the Nankai Trough, there is a major along-strike transition from deeper interseismic coupling beneath Shikoku (∼30 km depth [e.g., *Mazzotti et al.*, 2000; *Ito and Hashimoto*, 2004]) to a shallow downdip termination of interseismic coupling offshore of the Kyushu region (<20 km [*Nishimura and Hashimoto*, 2006; *Wallace et al.*, 2009]) on the Ryukyu Trench. Like the Hikurangi margin, this along-strike change from deep to shallow coupling accompanies an abrupt change from long-term upper plate trans-

pression (Shikoku and southwest Honshu) to upper plate transtension (Kyushu). The lateral transition from deep to shallow coupling in southwest Japan occurs beneath the Bungo Channel, where a large slow slip event was documented in 1996 [*Hirose et al.*, 1999]. The Bungo Channel slow slip event was similar in size, depth, and duration to the Manawatu event that occurred in the lateral transition zone from deep to shallow interseismic coupling at the Hikurangi margin. Strong along-strike variations in the depth of interseismic coupling are also observed on the megathrust offshore Alaska [*Freymueller et al.*, 2008] and adjacent to the Aleutian arc, near the Shumagin Islands [*Fournier and Freymueller*, 2007] and the Andreanof Islands [*Cross and Freymueller*, 2007]. However, we note that these strong along-strike variations in interseismic coupling in Alaska are not accompanied by clear along-strike changes from upper plate contraction to upper plate extension, unlike the Nankai/Ryukyu and Hikurangi margins.

[52] Aspects of the seismogenic zone beneath the southern North Island may be analogous to some portions of the northern Japan Trench. Deep interseismic coupling occurs beneath parts of northern Japan (50–60 km deep [*Mazzotti et al.*, 2000] and possibly as deep as 100 km depth [*Suwa et al.*, 2006]). Such deep interseismic coupling has been attributed to subduction of Cretaceous oceanic crust, which depresses the thermal structure of the subduction interface, causing the 350°C isotherm to be reached at deeper levels than in most other subduction margins [e.g., *Wang and Suyehiro*, 1999]. Like the Hikurangi margin, there are along-strike variations in the depth of the downdip limit of interseismic coupling on the Japan Trench [*Mazzotti et al.*, 2000; *Suwa et al.*, 2006] and considerable spatial variation of asperities inferred from historic subduction thrust events [*Yamanaka and Kikuchi*, 2004].

[53] Geodetic data suggest that the downdip limit of interseismic coupling adjacent to the Nicoya Peninsula, Costa Rica, occurs just offshore, at ∼12–16 km depth [*Norabuena et al.*, 2004], comparable to the downdip limit of interseismic coupling offshore of the central and northern portion of the Hikurangi margin. *Spinelli and Saffer* [2004] conducted thermal modeling of the subduction margin in the Nicoya Peninsula region, and their results predict temperatures of ∼250°C in the region of the downdip limit of interseismic coupling estimated from geodetic studies [*Norabuena et al.*, 2004; *DeShon et al.*, 2006], only slightly higher than temperatures obtained by *McCaffrey et*

al. [2008] at the downdip limit of interseismic coupling in the northern and central Hikurangi margin (Figure 9) and similar to temperatures obtained by *Fagereng and Ellis* [2009] for their case with high shear stress on the interface. The downdip limit of interseismic coupling (and possibly, the seismogenic zone) beneath the Nicoya Peninsula and the central and northern Hikurangi margin do not appear to be controlled by the depth to the 350°C isotherm in contrast to what has been proposed for other subduction margins [e.g., *Oleskevich et al.*, 1999]. Like the northern Hikurangi margin, the Costa Rica margin is also characterized by subduction erosion processes [*Ranero and von Huene*, 2000], and such processes are thought to influence fluid pressures and material properties at the subduction thrust decollement, and could play a role in the distribution of subduction thrust earthquakes [e.g., *von Huene et al.*, 2004]. Fluid pressures, upper plate structure, degree of subduction erosion, dewatering of the subducted plate, and seamount subduction, among other factors, are all thought to play roles in the distribution of seismicity and interseismic coupling at the Costa Rica margin [e.g., *Bilek et al.*, 2003; *DeShon et al.*, 2006].

5. Conclusions

[54] In the absence of historical great subduction thrust events, we use geophysical and geological data to characterize the seismogenic zone of the Hikurangi subduction thrust. The probable seismogenic zone and the physical properties of the Hikurangi subduction margin show major along-strike variations (Figures 4, 5, 10, and 12–14). The southern portion of the margin contains a well-developed accretionary wedge (Figure 4a), and is the site of a broad zone of deep interseismic coupling at the subduction interface (see summary in Figure 14c). Most of the upper plate in the onshore portion of the southern margin undergoes substantial long-term tectonic contraction. Fluid overpressure may be efficiently maintained in the compressional environment, leading to a low shear strength, but fully coupled plate interface. The southern portion of the margin may be capable of producing great subduction thrust events as large as $M_W \sim 8.2–8.7$ (see Appendix B).

[55] The northern and central parts of the margin are impacted by subducting seamounts, undergo frontal subduction erosion (in places), have a less pronounced accretionary wedge (Figures 1, 4b, and 4c), shallow interseismic coupling, a mildly extensional upper plate in the Raukumara peninsula portion of the fore arc, and a zone of high Vp/Vs and low Qp near the interface and within the upper plate indicative of high fluid volumes (see summary in Figures 14a and 14b). Hydrofracture triggered by local overpressure, as well as movement in episodic slow slip events may enhance structural permeability, thus influencing fluid pressures within the upper plate and near the interface. This portion of the megathrust may be characterized by more frequent, moderate-magnitude earthquakes (in contrast to the southern part of the Hikurangi margin, where we expect larger events), but we cannot rule out the occurrence of great subduction thrust events here, particularly in the Hawke's Bay region (see Appendix B).

[56] Although great advances have been made in our understanding of the Hikurangi margin over the last decade, we are only beginning to understand the physical processes that may dictate the likely rupture areas of future earthquakes at the Hikurangi margin. To develop a coherent physical model for Hikurangi margin seismogenesis, better heat flow data, accurate measurements of fluid pressure conditions, more paleoseismological studies searching for prehistoric interface ruptures, additional active and passive seismic surveys, offshore geodetic measurements, and ongoing collection of continuous and campaign GPS data are all needed. The major along-strike variations in subduction thrust processes that we observe in New Zealand thus far suggest that the seismogenic behavior of the Hikurangi subduction thrust cannot be explained using only one or two simple parameters. We suggest that an interplay between factors such as upper and lower plate structure, regional tectonic stresses (extensional versus contractional), sediment subduction, and fluid pressures have a major influence on seismogenic processes at the Hikurangi margin, and are probably more important than thermal effects. It is likely that subduction zone seismogenesis elsewhere is dictated by complex feedbacks between numerous processes, and some of our long-held assumptions about subduction margins worldwide may require reevaluation.

Appendix A: Terminology and Theoretical Quantities Relevant to the Discussion of Subduction Zone Seismogenesis

[57] In order to discuss the Hikurangi margin's seismogenic potential, it is helpful to define some concepts invoked throughout this review. The term

"coupling" is widely used in the literature to describe a variety of fault zone and plate boundary processes, and great confusion surrounds the meaning of this term [*Wang and Dixon*, 2004; *Lay and Schwartz*, 2004]. The term "interseismic coupling" here refers to the relative motion between adjacent rocks on either side of a fault in the time between large magnitude earthquakes on that fault. Interseismic coupling is typically represented by a purely kinematic quantity we call the interseismic coupling coefficient, $\phi_{ic} = 1 - (V_c/V)$, where V is the long-term averaged slip rate on the fault (over many earthquake cycles) and V_c the short-term creep rate. If $\phi_{ic} = 0$ then this region of the fault is creeping at the full long-term slip rate and if $\phi_{ic} = 1$ there is no creep in the interseismic period. In the case where ϕ_{ic} is neither 0 nor 1, one could interpret it as a spatial and/or temporal average of creeping and noncreeping patches [*Scholz*, 1990; *Lay and Schwartz*, 2004]. The slip rate deficit vector on the fault is the scalar coupling value ϕ multiplied by the relative motion vector V between the two blocks at a given point on a fault. The slip rate deficit is the amount of equivalent fault "slip" that is accumulating as elastic strain in the region surrounding the fault. Presumably this accumulated slip deficit will eventually be recovered as slip on the fault in an earthquake, or in a slow slip event.

[58] Numerous expressions have been devised to describe the frictional behavior of fault zone material. "Velocity-strengthening" and "velocity-weakening" behavior refer to the increase or decrease, respectively, in the dynamic coefficient of friction as the slip velocity on a fault increases (e.g., during an earthquake) [e.g., *Scholz*, 1998]. Velocity-strengthening (frictionally stable) materials therefore tend not to support rapid earthquake slip, and often exhibit creep behavior, while velocity-weakening (frictionally unstable) zones tend to exhibit stick-slip type behavior [e.g., *Scholz*, 1990, 1998]. More viscous materials exhibit velocity strengthening behavior, making temperature a possible control on stick-slip versus stable sliding behavior. Poorly consolidated sediments also tend to be velocity strengthening [e.g., *Scholz*, 1990]. "Conditionally" stable [*Scholz*, 1990] materials are thought to slip aseismically at normal interplate strain rates (stable), but can become velocity weakening at extremely high strain rates allowing earthquake rupture to propagate into the conditionally stable field [e.g., *Hyndman et al.*, 1997, and references therein]. Conditional stability is often suggested to occur in a transition zone between velocity weakening and velocity strengthening regimes [e.g., *Hyndman and Wang*, 1993].

Appendix B: Rupture Segments and Potential Earthquake Magnitudes at the Hikurangi Margin

[59] Given that the moment of an earthquake is proportional to the area of the fault that slips in the event, knowledge of possible rupture segmentation scenarios are critical for anticipating the seismic hazard posed by a subduction zone. Coupled regions on the plate interface capable of producing large thrust events may rupture the same area repeatedly [e.g., *Thatcher*, 1990], as in the case of the northeast Japan subduction zone [*Yamanaka and Kikuchi*, 2004]. Typically the boundaries between these regions are controlled by structures on the subducted plate, such as large seamounts or ridges [e.g., *Kodaira et al.*, 2002, 2006], or by structures in the upper plate [e.g., *Collot et al.*, 2004]. However, there could be any number of potential rupture segments and sizes that rupture individually, or cascade into larger ruptures depending on initial stress conditions, nucleation and dynamic rupture properties.

[60] GPS and seismological data collected to date provide no reliable information regarding the updip termination of any potential subduction interface ruptures at the Hikurangi margin, which has an impact on our estimates of possible earthquake magnitudes that the Hikurangi margin can produce. Despite these uncertainties in the updip limit, it is worth noting that the boundary between the deforming accretionary wedge and the buttress of Cretaceous and Paleogene rocks (Figure 1, boundary shown with a dashed white line) may be a possible candidate for the updip termination of rupture in some subduction thrust events. However, we cannot rule out other scenarios such as rupture all the way to the trench, or updip termination of rupture deeper or shallower than the wedge/buttress boundary.

[61] Although the historical record of subduction interface earthquakes at the Hikurangi margin is not sufficient to delineate potential rupture segments, we can make some educated assessments of the geometry of these segments. The broad zone of strong interseismic coupling in the lower North Island may constitute a southern North Island segment (Figure B1). The slip rate deficit on the subduction interface becomes very low in the model of *Wallace et al.* [2004] beneath Cook Strait
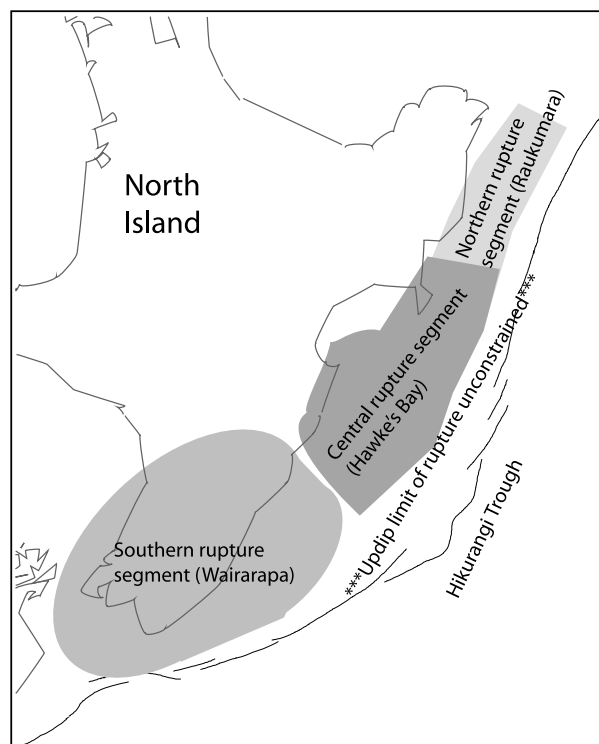
Figure B1. Schematic showing generalized rupture regions for possible subduction earthquake events discussed in Appendix B. Note that the updip limit of rupture in each case is unknown.

and the northern South Island, increasing the likelihood that the southern termination of a subduction interface earthquake would occur near or just to the south of Cook Strait (Figure 6). The northeastern boundary of this segment probably occurs at the very marked change in width of the coupled zone near Cape Turnagain (Figures 6 and B1). This rupture segment is ~230 km long and 150–185 km wide, depending on the updip rupture limit assumed. If the scaling relationships between fault area and seismic moment proposed by *Abe* [1975] are reasonable, such a segment may rupture in an M_w 8.5–8.7 event, with 8–12 m of slip (assuming a 3–5 MPa stress drop and crustal rigidities of 3 × 10^{10} N/m²). Given that the current slip rate deficit on the lower North Island segment is 20–25 mm/yr, the average recurrence interval of such an event could be ~300–625 years. However, it is possible that slip may occur on the subduction interface in more frequent, smaller events, or as afterslip for years to decades following a major rupture, leading to recovery of an even greater proportion of the slip rate deficit and resulting in longer intervals between major earthquake events.

[62] The temporal correlation between one of the coastal subsidence events observed in southern and northern Hawke's Bay at ~7 ka [*Cochran et al.*, 2006; *Hayward et al.*, 2006] suggests that rupture of the central segment of the subduction interface (Hawke's Bay segment; Figure B1) is a likely scenario. To explain the observed subsidence at core sites in northern Hawke's Bay (Figures 7 and 8), a model where simultaneous rupture (~8 m of slip) of the subduction thrust and the Lachlan Fault (a splay fault, Figure 1), equivalent to an $M_w \sim$ 8.1 event, was proposed [*Cochran et al.*, 2006]. If we assume rupture of the entire Hawke's Bay segment (180 km by 90 km wide), an M_w 8.3 event on the subduction thrust would result (assuming 8 m of slip on the interface, equivalent to a 5 MPa stress drop). It is possible that the Hawke Bay segment continues northward to the northeast Hikurangi margin (Raukumara segment; Figure B1), as the interseismic coupling distributions in both locations share similar characteristics (shallow downdip limit of coupling; Figure 6). Simultaneous rupture of the Raukumara and Hawke's Bay segments (~400 km long by 90 km wide) involving ~8 m slip could produce an $M_w \sim$ 8.6 earthquake.

[63] The surface of the incoming plate at the northeast Hikurangi margin is studded with seamounts, and can thus be characterized as rough, and conducive to the occurrence of "tsunami earthquakes" [e.g., *Satake and Tanioka*, 1999] on the shallow part of the plate interface near the trench. The M_W 7.0–7.1 25 March and M_W 6.9–7.1 17 May 1947 East Coast Gisborne earthquakes had long source durations, consistent with being a "slow" or "tsunami" earthquake [*Downes et al.*, 2000]. The margin-normal convergence rate at the trench in this region is ~55 mm/yr [*Wallace et al.*, 2004]. Assuming a coupling coefficient of 1.0 at the asperities and average slip of 4 m for the 1947 events [*Downes et al.*, 2000] we would thus expect tsunami earthquakes similar to those in 1947 to recur every ~70 years. Interestingly, recent searching of historical data has revealed evidence of an earthquake in 1880 (possibly in a similar location to the 1947 events) with some of the characteristics one would expect for a tsunami earthquake. In particular, it was only mildly felt and was followed by a tsunami that was identified by the presence of dead fish above the high tide mark (G. Downes, unpublished data, 2007). If it was a tsunami earthquake in the same location as the 1947 event, the return time would be close to 70 years in this case.

[64] Lessons from the 2004 Sumatra earthquake demand that we consider the possibility of rupture of the entire Hikurangi margin in a single earthquake, where increased strain rate at rupture tips may lead to rupture propagation into normally creeping segments. This could produce an earthquake $>M_w$ 8.8, rupturing a region of the subduction interface >650 km long by 100 km wide, with 10 m (or more) slip on the subduction thrust. An even more serious scenario would involve simultaneous rupture of the entire Hikurangi-Kermadec Trench; such an event would be similar in scale (~1500 km rupture length) to the 2004 Sumatra event. Large magnitude earthquakes ($M_w \sim 7.5$) have been documented at the northern end of the Kermadec Trench/southern end of the Tonga Trench [*Christensen and Lay*, 1988], and the velocity of a GPS site at Raoul Island (Figure 1) (L. M. Wallace unpublished data, 2007) indicates that there may be some interseismic coupling on the subduction thrust in the central portion of the Kermadec Trench. However, like the Andaman margin prior to 26 December 2004, the seismogenic potential of the Kermadec Trench is not well known.

Acknowledgments

References

Abe, K. (1975), Reliable estimation of the seismic moment of large earthquakes, *J. Phys. Earth*, *23*, 381–390.

Abercrombie, R. E., and R. A. Benites (1998), Strong motion modelling of the 1993 Tikokino earthquake, southern Hawke's Bay, New Zealand, *N. Z. J. Geol. Geophys.*, *41*(3), 259–270.

Allis, R. G., R. Funnel, and X. Zhan (1998), From basin to mountains and back again: NZ basin evolution since 10 Ma, in *WR19: Proceedings of the 9th International Symposium on Water-Rock Interaction, Taupo, NZ, 30 March–3 April*, pp. 3–10, A. A. Balkema, Rotterdam, Netherlands.

Ansell, J., and S. Bannister (1996), Shallow morphology of the subducted Pacific Plate along the Hikurangi margin, New Zealand, *Phys. Earth Planet. Inter.*, *93*, 3–20, doi:10.1016/0031-9201(95)03085-9.

Arnadóttir, T., S. Thornley, F. Pollitz, and D. Darby (1999), Spatial and temporal strain rate variations at the northern Hikurangi margin, New Zealand, *J. Geophys. Res.*, *104*, 4931–4944, doi:10.1029/1998JB900109.

Atwater, B. F. (1987), Evidence for great Holocene earthquakes along the outer coast of Washington State, *Science*, *236*, 942–944, doi:10.1126/science.236.4804.942.

Bangs, N. L. B., S. P. S. Gulick, and T. H. Shipley (2006), Seamount subduction erosion in the Nankai Trough and its potential impact on the seismogenic zone, *Geology*, *34*(8), 701–704, doi:10.1130/G22451.1.

Bannister, S. (1986), Seismicity, stress field and lithospheric structure of the northern Hawke's Bay region, New Zealand, Ph.D. thesis, Victoria Univ. of Wellington, Wellington.

Barker, D. H. N., R. Sutherland, S. Henrys, and S. Bannister (2009), Geometry of the Hikurangi subduction thrust and upper plate, North Island, New Zealand, *Geochem. Geophys. Geosyst.*, *10*, Q02007, doi:10.1029/2008GC002153.

Barnes, P. M., and B. Mercier de Lepinay (1997), Rates and mechanics of rapid frontal accretion along the very obliquely convergent southern Hikurangi margin, New Zealand, *J. Geophys. Res.*, *102*(B11), 24,931–24,952, doi:10.1029/97JB01384.

Barnes, P. M., and A. Nicol (2004), Formation of an active thrust triangle zone associated with structural inversion in a subduction setting, eastern New Zealand, *Tectonics*, *23*, TC1015, doi:10.1029/2002TC001449.

Barnes, P. M., B. Mercier de Lépinay, J.-Y. Collot, J. Delteil, and J.-C. Audru (1998a), Strain partitioning in the transition area between oblique subduction and continental collision, Hikurangi margin, New Zealand, *Tectonics*, *17*(4), 534–557, doi:10.1029/98TC00974.

Barnes, P. M., B. Mercier de Lépinay, J.-Y. Collot, J. Delteil, J.-C. Audru, and GeodyNZ Team (1998b), South Hikurangi GeodyNZ swath maps: Depths, texture and geological interpretation, scale 1:500000, *N. Z. Oceanogr. Inst. Chart, Misc. Ser. 75*, Natl. Inst. of Water and Atmos. Res., Wellington.

Barnes, P. M., A. Nicol, and T. Harrison (2002), Late Cenozoic evolution and earthquake potential of an active listric thrust complex above the Hikurangi subduction zone, New Zealand, *Geol. Soc. Am. Bull.*, *114*(11), 1379–1405, doi:10.1130/0016-7606(2002)114<1379:LCEAEP>2.0.CO;2.

Barnes, P. M., G. Lamarche, J. Bialas, I. Pecher, S. Henrys, G. Netzeband, J. Greinert, J. Mountjoy, K. Pedley, and G. Crutchley (2009), Tectonic and Geological framework for gas hydrates and cold seeps on the Hikurangi subduction margin, New Zealand, *Mar. Geol.*, doi:10.1016/j.margeo.2009.03.012, in press.

Beanland, S., and J. Haines (1998), The kinematics of active deformation in the North Island, New Zealand, determined from geological strain rates, *N. Z. J. Geol. Geophys.*, *41*, 311–323.

Beavan, R. J., and D. J. Darby (2005), Fault slip in the 1855 Wairarapa earthquake based on new and reassessed vertical motion observations: Did slip occur on the subduction interface?, in *The 1855 Wairarapa Earthquake Symposium: 150 Years of Thinking About Magnitude 8+ Earthquakes and Seismic Hazard in New Zealand: 8–10 September 2005: Proceedings Volume*, edited by J. Townend, R. M. Langridge, and A. Jones, pp. 31–41, Greater Wellington Reg. Counc., Wellington.

Beavan, J., and J. Haines (2001), Contemporary horizontal velocity and strain-rate fields of the Pacific-Australian plate boundary zone through New Zealand, *J. Geophys. Res.*, *106*(B1), 741–770, doi:10.1029/2000JB900302.

Beavan, J., P. Tregoning, M. Bevis, T. Kato, and C. Meertens (2002), Motion and rigidity of the Pacific Plate and implications for plate boundary deformation, *J. Geophys. Res.*, *107*(B10), 2261, doi:10.1029/2001JB000282.

Beavan, J., L. Wallace, A. Douglas, and H. Fletcher (2007), Slow slip events on the Hikurangi subduction interface, New Zealand, in *Monitoring and Understanding a Dynamic*

Planet With Geodetic and Oceanographic Tools, IAG Symposium, Cairns, Australia, 22–26 August, 2005, Int. Assoc. of Geod. Symp., vol. 130, edited by P. Tregoning and C. Rizos, pp. 438–444, Springer, Berlin.

Beavan, R. J., L. M. Wallace, and R. McCaffrey (2008), Recurring slow slip on the Hikurangi subduction interface, New Zealand, *Eos Trans. AGU*, *89*(53), Fall Meet. Suppl., Abstract U31B-04.

Behrmann, J. H. (1991), Conditions of hydrofracture and the fluid permeability of accretionary wedges, *Earth Planet. Sci. Lett.*, *107*, 550–558, doi:10.1016/0012-821X(91)90100-V.

Berryman, K. (1993), Age, height and deformation of Holocene marine terraces at Mahia Peninsula, Hikurangi subduction margin, New Zealand, *Tectonics*, *12*(6), 1347–1364, doi:10.1029/93TC01542.

Berryman, K. R., Y. Ota, and A. G. Hull (1989), Holocene paleoseismicity in the fold and thrust belt of the Hikurangi subduction zone, eastern North Island, New Zealand, *Tectonophysics*, *163*, 185–195, doi:10.1016/0040-1951(89)90256-4.

Bilek, S., S. Y. Schwartz, and H. DeShon (2003), Control of seafloor roughness on earthquake rupture behavior, *Geology*, *31*(5), 455–458, doi:10.1130/0091-7613(2003)031<0455:COSROE>2.0.CO;2.

Blanpied, M. L., D. A. Lockner, and J. D. Byerlee (1991), Fault stability inferred from granite sliding experiments at hydrothermal conditions, *Geophys. Res. Lett.*, *18*, 609–612, doi:10.1029/91GL00469.

Cashman, S. M., H. M. Kelsey, C. F. Erdman, H. N. C. Cutten, and K. R. Berryman (1992), Strain partitioning between structural domains in the forearc of the Hikurangi subduction zone, New Zealand, *Tectonics*, *11*, 242–257, doi:10.1029/91TC02363.

Chlieh, M., J. B. de Chabalier, J. C. Ruegg, R. Armijo, R. Dmowska, J. Campos, and K. L. Feigl (2004), Crustal deformation and fault slip during the seismic cycle in the North Chile subduction zone, from GPS and InSAR observations, *Geophys. J. Int.*, *158*, 695–711, doi:10.1111/j.1365-246X.2004.02326.x.

Chlieh, M., J. P. Avouac, K. Sieh, D. H. Natawidjaja, and J. Galetzka (2008), Heterogeneous coupling of the Sumatran megathrust constrained by geodetic and paleogeodetic measurements, *J. Geophys. Res.*, *113*, B05305, doi:10.1029/2007JB004981.

Christensen, D., and T. Lay (1988), Large earthquakes in the Tonga region associated with subduction of the Louisville Ridge, *J. Geophys. Res.*, *93*, 13,367–13,389, doi:10.1029/JB093iB11p13367.

Cisternas, M., et al. (2005), Predecessors of the giant 1960 Chile earthquake, *Nature*, *437*, 404–407, doi:10.1038/nature03943.

Clague, J. J. (1997), Evidence for large earthquakes at the Cascadia subduction zone, *Rev. Geophys.*, *35*, 439–460, doi:10.1029/97RG00222.

Cloos, M. (1992), Thrust-type subduction zone earthquakes and seamount asperities: A physical model for earthquake rupture, *Geology*, *20*, 601–604, doi:10.1130/0091-7613(1992)020<0601:TTSZEA>2.3.CO;2.

Cloos, M., and R. L. Shreve (1988a), Subduction-channel model of prism accretion, melange formation, sediment subduction, and subduction erosion at convergent plate margins: 1. Background and description, *Pure Appl. Geophys.*, *128*, 455–500, doi:10.1007/BF00874548.

Cloos, M., and R. L. Shreve (1988b), Subduction-channel model of prism accretion, melange formation, sediment subduction, and subduction erosion at convergent plate margins: 2. Implications and discussion, *Pure Appl. Geophys.*, *128*, 501–545, doi:10.1007/BF00874549.

Cochran, U. A., et al. (2006), Paleoecological insights into subduction zone earthquake occurrence, eastern North Island, New Zealand, *Geol. Soc. Am. Bull.*, *118*, 1051–1074, doi:10.1130/B25761.1.

Collot, J.-Y., et al. (1996), From oblique subduction to intra-continental transpression: Structures of the southern Kermadec-Hikurangi margin from multibeam bathymetry, side-scan sonar and seismic reflection, *Mar. Geophys. Res.*, *18*, 357–381, doi:10.1007/BF00286085.

Collot, J.-Y., K. Lewis, G. Lamarche, and S. Lallemand (2001), The giant Ruatoria debris avalanche on the northern Hikurangi margin, New Zealand: Result of oblique seamount subduction, *J. Geophys. Res.*, *106*(B9), 19,271–19,297, doi:10.1029/2001JB900004.

Collot, J.-Y., B. Marcaillou, F. Sage, F. Michaud, W. Agudelo, P. Charvis, D. Graindorge, M.-A. Gutscher, and G. Spence (2004), Are rupture zone limits of great subduction earthquakes controlled by upper plate structures? Evidence from multichannel seismic reflection data acquired across the northern Ecuador–southwest Colombia margin, *J. Geophys. Res.*, *109*, B11103, doi:10.1029/2004JB003060.

Cross, R. S., and J. T. Freymueller (2007), Plate coupling variation and block translation in the Andreanof segment of the Aleutian arc determined by subduction modeling using GPS data, *Geophys. Res. Lett.*, *34*, L06304, doi:10.1029/2006GL028970.

Currie, C. A., R. D. Hyndman, K. Wang, and V. Kostoglodov (2002), Thermal models of the Mexico subduction zone: Implications for the megathrust seismogenic zone, *J. Geophys. Res.*, *107*(B12), 2370, doi:10.1029/2001JB000886.

Darby, D. J., and S. Beanland (1992), Possible source models for the 1855 Wairarapa Earthquake, New Zealand, *J. Geophys. Res.*, *97*, 12,375–12,389, doi:10.1029/92JB00567.

Darby, D., and J. Beavan (2001), Evidence from GPS measurements for contemporary interplate coupling on the southern Hikurangi subduction thrust and for partitioning of strain in the upper plate, *J. Geophys. Res.*, *106*, 30,881–30,891, doi:10.1029/2000JB000023.

Davey, F. J., and E. G. C. Smith (1983), A crustal seismic reflection-refraction experiment across the subducted Pacific Plate under Wellington, New Zealand, *Phys. Earth Planet. Inter.*, *31*(4), 327–333, doi:10.1016/0031-9201(83)90092-4.

Davey, F. J., M. Hampton, J. Childs, M. A. Fisher, K. Lewis, and J. R. Pettinga (1986), Structure of a growing accretionary prism, Hikurangi margin, New Zealand, *Geology*, *14*, 663–666, doi:10.1130/0091-7613(1986)14<663:SOAGAP>2.0.CO;2.

Davis, D. J., J. Suppe, and F. A. Dahlen (1983), Mechanics of fold-and-thrust belts and accretionary wedges, *J. Geophys. Res.*, *88*, 1153–1172, doi:10.1029/JB088iB02p01153.

Davy, B., and R. Wood (1994), Gravity and magnetic modelling of the Hikurangi Plateau, *Mar. Geol.*, *118*, 139–151, doi:10.1016/0025-3227(94)90117-1.

Davy, B. R., K. Hoernle, and R. Werner (2008), Hikurangi Plateau: Crustal structure, rifted formation, and Gondwana subduction history, *Geochem. Geophys. Geosyst.*, *9*, Q07004, doi:10.1029/2007GC001855.

Delahaye, E. J. (2008), Seismic tremor and small earthquakes associated with slow slip in the Hikurangi subduction zone, M.Sc. thesis, Victoria Univ. of Wellington, Wellington.

Delahaye, E. J., J. Townend, M. E. Reyners, and G. Rodgers (2009), Microseismicity but no tremor accompanying slow

slip in the Hikurangi subduction zone, New Zealand, *Earth Planet. Sci. Lett.*, *277*, 21–28, doi:10.1016/j.epsl.2008.09.038.

DeShon, H. R., S. Y. Schwartz, A. V. Newman, V. González, M. Protti, L. M. Dorman, T. H. Dixon, D. H. Sampson, and E. R. Flueh (2006), Seismogenic zone structure beneath the Nicoya Peninsula, Costa Rica, from three-dimensional local earthquake *P*- and *S*-wave tomography, *Geophys. J. Int.*, *164*(1), 109–124, doi:10.1111/j.1365-246X.2005.02809.x.

Doser, D. I., and T. H. Webb (2003), Source parameters of large historical (1917–1961) earthquakes, North Island, New Zealand, *Geophys. J. Int.*, *152*, 795–832, doi:10.1046/j.1365-246X.2003.01895.x.

Douglas, A., J. Beavan, L. Wallace, and J. Townend (2005), Slow slip on the northern Hikurangi subduction interface, New Zealand, *Geophys. Res. Lett.*, *32*, L16305, doi:10.1029/2005GL023607.

Downes, G. L. (2006), The 1904 M$_S$6.8 M$_w$ 7.0–7.2 Cape Turnagain, New Zealand, earthquake, *Bull. N. Z. Soc. Earthquake Eng.*, *39*(4), 182–207.

Downes, G., T. H. Webb, M. J. McSaveney, C. Chague-Goff, D. J. Darby, and A. Barnett (2000), The March 25 and May 17 1947 Gisborne earthquakes and tsunami: Implication for tsunami hazard for East Coast, North Island, New Zealand, paper presented at Joint IOC/IUGG International Workshop: Tsunami Risk Assessment Beyond 2000—Theory, Practice and Plans, Intergov. Oceanogr. Comm., Moscow, 14–16 June.

Dowrick, D. J., and D. A. Rhoades (1998), Magnitudes of New Zealand earthquakes, 1901–1993, *Bull. N. Z. Soc. Earthquake Eng.*, *31*, 260–280.

Dragert, H., K. Wang, and T. James (2001), A silent slip event on the deeper Cascadia subduction interface, *Science*, *292*, 1525–1528, doi:10.1126/science.1060152.

Eberhart-Phillips, D., and M. Chadwick (2002), Three-dimensional attenuation model of the shallow Hikurangi subduction zone in the Raukumara Peninsula, New Zealand, *J. Geophys. Res.*, *107*(B2), 2033, doi:10.1029/2000JB000046.

Eberhart-Phillips, D., and M. Reyners (1997), Continental subduction and three-dimensional crustal structure: The northern South Island, New Zealand, *J. Geophys. Res.*, *102*, 11,843–11,861, doi:10.1029/96JB03555.

Eberhart-Phillips, D., and M. Reyners (1999), Plate interface properties in the northeast Hikurangi subduction zone, New Zealand, from converted seismic waves, *Geophys. Res. Lett.*, *26*, 2565–2568, doi:10.1029/1999GL900567.

Eberhart-Phillips, D., D.-H. Han, and M. D. Zoback (1989), Empirical relationships among seismic velocity, effective pressure, porosity, and clay content in sandstone, *Geophysics*, *54*, 82–89, doi:10.1190/1.1442580.

Eberhart-Phillips, D., M. Reyners, M. Chadwick, and J.-M. Chiu (2005), Crustal heterogeneity and subduction processes: 3-D Vp, Vp/Vs and Q in the southern North Island, New Zealand, *Geophys. J. Int.*, *162*(1), 270–288, doi:10.1111/j.1365-246X.2005.02530.x.

Eberhart-Phillips, D., M. Reyners, M. Chadwick, and G. Stuart (2008), Three-dimensional attenuation structure of the Hikurangi subduction zone in the central North Island, New Zealand, *Geophys. J. Int.*, *174*(1), 418–434, doi:10.1111/j.1365-246X.2008.03816.x.

Fagereng, A., and S. Ellis (2009), On factors controlling the depth of interseismic coupling on the Hikurangi subduction interface, New Zealand, *Earth Planet. Sci. Lett.*, *278*, 120–130, doi:10.1016/j.epsl.2008.11.033.

Fournier, T. J., and J. T. Freymueller (2007), Transition from locked to creeping subduction in the Shumagin region,

Alaska, *Geophys. Res. Lett.*, *34*, L06303, doi:10.1029/2006GL029073.

Francoiş-Holden, C., et al. (2008), The M$_W$ 6.6 Gisborne Earthquake of 2007: Preliminary records and general source characterisation, *Bull. N. Z. Soc. Earthquake Eng.*, *41*(4), 266–277.

Freymueller, J. T., H. Woodard, S. Cohen, R. Cross, J. Elliott, C. Larsen, S. Hreinsdottir, and C. Zweck (2008), Active deformation processes in Alaska, based on 15 years of GPS measurements, in *Active Tectonics and Seismic Potential of Alaska*, *Geophys. Monogr. Ser.*, vol. 179, edited by J. T. Freymueller et al., pp. 1–42, AGU, Washington, D. C.

Fukao, Y. (1979), Tsunami earthquakes and subduction processes near deep-sea trenches, *J. Geophys. Res.*, *84*, 2303–2314, doi:10.1029/JB084iB05p02303.

Giggenbach, W. F., Y. Sano, and H. Wakita (1993), Isotopic composition of helium, and CO$_2$ and CH$_4$ contents in gases produced along the New Zealand part of a convergent plate boundary, *Geochim. Cosmochim. Acta*, *57*, 3427–3455, doi:10.1016/0016-7037(93)90549-C.

Grapes, R., and G. Downes (1997), The 1855 Wairarapa, New Zealand, earthquake: Analysis of historical data, *Bull. N. Z. Soc. Earthquake Eng.*, *30*(4), 271–368.

Hashimoto, C., A. Noda, T. Sagiya, and M. Matsu'ura (2009), Interplate seismogenic zones along the Kuril–Japan trench inferred from GPS data inversion, *Nat. Geosci.*, *2*, 141–144, doi:10.1038/ngeo421.

Hayward, B. W., H. R. Grenfell, A. T. Sabaa, R. Carter, U. A. Cochran, J. H. Lipps, P. R. Shane, and M. S. Morley (2006), Micropaleontological evidence of large earthquakes in the past 7200 years in southern Hawke's Bay, New Zealand, *Quat. Sci. Rev.*, *25*, 1186–1207, doi:10.1016/j.quascirev.2005.10.013.

Henrys, S., M. Reyners, I. Pecher, S. Bannister, Y. Nishimura, and G. Maslen (2006), Kinking of the subducting slab by escalator normal faulting beneath the North Island of New Zealand, *Geology*, *34*, 777–780, doi:10.1130/G22594.1.

Henrys, S. A., et al. (2009), Variation of bottom-simulating reflection (BSR) strength in a high-flux methane province, Hikurangi margin, in *Natural Gas Hydrates: Energy Resource Potential and Associated Geologic Hazards*, *AAPG Spec. Publ.*, edited by T. Collett et al., Am. Assoc. of Pet. Geol., Tulsa, Okla., in press.

Hirose, H., K. Hirahara, F. Kimata, N. Fujii, and S. Miyazaki (1999), A slow thrust slip event following the two 1996 Hyuganada earthquakes beneath the Bungo Channel, southwest Japan, *Geophys. Res. Lett.*, *26*(21), 3237–3240, doi:10.1029/1999GL010999.

Howorth, R., and A. Ross (1980), Holocene tephrostratigraphy and chronology at Tiniroto, Cook County, in *Proceedings of Tephra Workshop, June 30th–July 1st 1980*, edited by R. Howorth et al., pp. 41–50, Victoria Univ. of Wellington, Wellington.

Hreinsdóttir, S., J. T. Freymueller, R. Bürgmann, and J. Mitchell (2006), Coseismic deformation of the 2002 Denali Fault earthquake: Insights from GPS measurements, *J. Geophys. Res.*, *111*, B03308, doi:10.1029/2005JB003676.

Hull, A. G. (1987), A late Holocene marine terrace on the Kidnappers Coast, North Island, New Zealand: Some implications for shore platform development processes and uplift mechanism, *Quat. Res.*, *28*, 183–195, doi:10.1016/0033-5894(87)90058-5.

Hyndman, R. D., and K. Wang (1993), Thermal constraints on the zone of major thrust earthquake failure: The Cascadia Subduction Zone, *J. Geophys. Res.*, *98*(B2), 2039–2060, doi:10.1029/92JB02279.

Hyndman, R. D., K. Wang, and M. Yamano (1995), Thermal constraints on the seismogenic portion of the southwestern Japan subduction thrust, *J. Geophys. Res.*, *100*, 15,373–15,392, doi:10.1029/95JB00153.

Hyndman, R. D., M. Yamano, and D. A. Oleskovich (1997), The seismogenic zone of subduction thrust faults, *Isl. Arc*, *6*, 244–260, doi:10.1111/j.1440-1738.1997.tb00175.x.

Ito, T., and M. Hashimoto (2004), Spatiotemporal distribution of interplate coupling in southwest Japan from inversion of geodetic data, *J. Geophys. Res.*, *109*, B02315, doi:10.1029/2002JB002358.

Kanamori, H. (1972), Mechanism of tsunami earthquakes, *Phys. Earth Planet. Inter.*, *6*, 346–359, doi:10.1016/0031-9201(72)90058-1.

Kanamori, H. (1986), Rupture process of subduction zone earthquakes, *Annu. Rev. Earth Planet. Sci.*, *14*, 293–322, doi:10.1146/annurev.ea.14.050186.001453.

Kao, H., S.-J. Shan, H. Dragert, G. Rogers, J. F. Cassidy, and K. Ramachandran (2005), A wide depth distribution of seismic tremors along the northern Cascadia margin, *Nature*, *436*, 841–844, doi:10.1038/nature03903.

Kelsey, H. M., S. M. Cashman, S. Beanland, and K. R. Berryman (1995), Structural evolution along the inner forearc of the obliquely convergent Hikurangi margin, New Zealand, *Tectonics*, *14*, 1–18, doi:10.1029/94TC01506.

Kodaira, S., E. Kurashimo, J.-O. Park, N. Takahashi, A. Nakanishi, S. Miura, T. Iwasaki, N. Hirata, K. Ito, and Y. Kaneda (2002), Structural factors controlling the rupture process of a megathrust earthquake at the Nankai trough seismogenic zone, *Geophys. J. Int.*, *149*(3), 815–835, doi:10.1046/j.1365-246X.2002.01691.x.

Kodaira, S., T. Hori, A. Ito, S. Miura, G. Fujie, J.-O. Park, T. Baba, H. Sakaguchi, and Y. Kaneda (2006), A cause of rupture segmentation and synchronization in the Nankai trough revealed by seismic imaging and numerical simulation, *J. Geophys. Res.*, *111*, B09301, doi:10.1029/2005JB004030.

Lamarche, G., J.-N. Proust, and S. D. Nodder (2005), Long-term slip rates and fault interactions under low contractional strain, Wanganui Basin, NZ, *Tectonics*, *24*, TC4004, doi:10.1029/2004TC001699.

Larson, K., A. Lowry, V. Kostoglodov, W. Hutton, O. Sanchez, K. Hudnut, and G. Suarez (2004), Crustal deformation measurements in Guerrero, Mexico, *J. Geophys. Res.*, *109*, B04409, doi:10.1029/2003JB002843.

Lay, T., and S. Y. Schwartz (2004), Comment on "Coupling semantics and science in earthquake research,", *Eos Trans. AGU*, *85*(36), 339–340, doi:10.1029/2004EO360003.

Lewis, K., and J. Pettinga (1993), The emerging, imbricate frontal wedge of the Hikurangi margin, in *South Pacific Sedimentary Basins*, *Sediment. Basins of the World*, vol. 2, edited by P. B. Ballance, pp. 225–250, Elsevier Sci., Amsterdam.

Lewis, K. B., J.-Y. Collot, B. W. Davy, J. Delteil, S. E. Lallemand, C. I. Uruski, and GeodyNZ Team (1997), North Hikurangi GeodyNZ swath maps: Depth, texture and geological interpretation, *NIWA Chart Misc. Ser.*, *72*, Natl. Inst. of Water and Atmos. Res., Wellington.

Lewis, K. B., J.-Y. Collot, and S. E. Lallemande (1998), The dammed Hikurangi Trough: A channel-fed trench blocked by subducting seamounts and their wake avalanches (New Zealand–France GeodyNZ Project), *Basin Res.*, *10*(4), 441–468, doi:10.1046/j.1365-2117.1998.00080.x.

Lin, F.-C., M. H. Ritzwoller, J. Townend, S. Bannister, and M. K. Savage (2007), Ambient noise Rayleigh wave tomography of New Zealand, *Geophys. J. Int.*, *170*(2), 649–666, doi:10.1111/j.1365-246X.2007.03414.x.

Litchfield, N. (2008), Using fluvial terraces to determine Holocene coastal erosion and Late Pleistocene uplift rates: An example from northwestern Hawke Bay, New Zealand, *Geomorphology*, *99*, 369–386, doi:10.1016/j.geomorph.2007.12.001.

Litchfield, N., S. Ellis, K. Berryman, and A. Nicol (2007), Insights into subduction-related uplift along the Hikurangi Margin, New Zealand, using numerical modeling, *J. Geophys. Res.*, *112*, F02021, doi:10.1029/2006JF000535.

Litchfield, N., K. Wilson, K. Berryman, and L. Wallace (2009), Fluvial terraces in the lower Pakarae river valley: Evidence for coseismic river incision and implications for coastal uplift mechanisms, *Mar. Geol.*, in press.

Little, T. A., and D. W. Rogers (2005), Co-seismic slip during the 1855 earthquake, southern Wairarapa Fault, New Zealand, in *The 1855 Wairarapa Earthquake Symposium, 8–10 September 2005, Proceedings Volume*, edited by J. Townend, R. Langridge, and A. Jones, pp. 4–28, Greater Wellington Reg. Counc., Wellington.

Liu, Y., and J. R. Rice (2007), Spontaneous and triggered aseismic deformation transients in a subduction fault model, *J. Geophys. Res.*, *112*, B09404, doi:10.1029/2007JB004930.

Liu, Y., A. M. Rubin, J. R. Rice, and P. Segall (2008), Role of fault dilatancy in subduction zone aseismic deformation transients and thrust earthquakes, *Eos Trans. AGU*, *89*(53), Fall Meet. Suppl., Abstract S34B-04.

Long, A. J., and I. Shennan (1994), Sea-level changes in Washington and Oregon and the "earthquake deformation cycle,", *J. Coastal Res.*, *10*, 825–838.

Mazzotti, S., X. LePichon, P. Henry, and S. Miyazaki (2000), Full interseismic locking of the Nankai and Japan-west Kurile subduction zones: An analysis of uniform elastic strain accumulation in Japan constrained by permanent GPS, *J. Geophys. Res.*, *105*(B6), 13,159–13,177, doi:10.1029/2000JB900060.

McCaffrey, R. (1993), On the role of the upper plate in great subduction zone earthquakes, *J. Geophys. Res.*, *98*(B7), 11,953–11,966, doi:10.1029/93JB00445.

McCaffrey, R. (1997), Influences of recurrence times and fault zone temperatures on the age-rate dependence of subduction zone seismicity, *J. Geophys. Res.*, *102*(B10), 22,839–22,854, doi:10.1029/97JB01827.

McCaffrey, R. (2002), Crustal block rotations and plate coupling, in *Plate Boundary Zones*, *Geodyn. Ser.*, vol. 30, edited by S. Stein and J. Freymueller, pp. 100–122, AGU, Washington, D. C.

McCaffrey, R. (2007), The next great earthquake, *Science*, *315*, 1675–1676, doi:10.1126/science.1140173.

McCaffrey, R., M. D. Long, C. Goldfinger, P. C. Zwick, J. L. Nabelek, C. K. Johnson, and C. Smith (2000), Rotation and plate locking at the southern Cascadia subduction zone, *Geophys. Res. Lett.*, *27*, 3117–3120, doi:10.1029/2000GL011768.

McCaffrey, R., L. M. Wallace, and J. Beavan (2008), Slow slip and frictional transition at low temperature at the Hikurangi subduction zone, *Nat. Geosci.*, *1*, 316–320, doi:10.1038/ngeo178.

Mitsui, Y., and K. Hirahara (2008), Long-term slow slip events are not necessarily caused by high pore fluid pressure at the plate interface: An implication from two-dimensional model calculations, *Geophys. J. Int.*, *174*, 331–335, doi:10.1111/j.1365-246X.2008.03832.x.

Miura, S., Y. Suwa, A. Hasegawa, and T. Nishimura (2004), The 2003 M8.0 Tokachi-Oki earthquake—How much has

the great event paid back slip debts?, *Geophys. Res. Lett.*, *31*, L05613, doi:10.1029/2003GL019021.

Mochizuki, K., T. Yamada, M. Shinohara, and Y. Yamanaka (2008), Weak interplate coupling by seamounts and Mw ∼7.0 earthquakes, *Science*, *321*, 1194–1197, doi:10.1126/science.1160250.

Moore, J. C., and D. Saffer (2001), Updip limit of the seismogenic zone beneath the accretionary prism of southwest Japan: An effect of diagenetic to low-grade metamorphic processes and increasing effective stress, *Geology*, *29*(2), 183–186, doi:10.1130/0091-7613(2001)029<0183:ULOTSZ>2.0.CO;2.

Mortimer, N. (2004), New Zealand's geological foundations, *Gondwana Res.*, *7*, 261–272, doi:10.1016/S1342-937X(05)70324-5.

Mortimer, N., and D. Parkinson (1996), Hikurangi Plateau: A Cretaceous large igneous province in the southwest Pacific Ocean, *J. Geophys. Res.*, *101*(B1), 687–696, doi:10.1029/95JB03037.

Mumme, T. C., S. H. Lamb, and R. I. Walcott (1989), The Raukumara paleomagnetic domain: Constraints on the tectonic rotation of the east coast, North Island, New Zealand, from paleomagnetic data, *N. Z. J. Geol. Geophys.*, *32*, 317–326.

Nadeau, R. M., and T. M. McEvilly (2004), Periodic pulsing of characteristic microearthquakes on the San Andreas Fault, *Science*, *303*, 220–222, doi:10.1126/science.1090353.

Nicol, A., and J. Beavan (2003), Shortening of an overriding plate and its implications for slip on a subduction thrust, central Hikurangi Margin, New Zealand, *Tectonics*, *22*(6), 1070, doi:10.1029/2003TC001521.

Nicol, A., and L. M. Wallace (2007), Temporal stability of deformation rates: Comparison of geological and geodetic observations, Hikurangi subduction margin, New Zealand, *Earth Planet. Sci. Lett.*, *258*, 397–413, doi:10.1016/j.epsl.2007.03.039.

Nicol, A., C. Mazengarb, F. Chanier, G. Raitt, C. Uruski, and L. Wallace (2007), Tectonic evolution of the active Hikurangi subduction margin, New Zealand, since the Oligocene, *Tectonics*, *26*, TC4002, doi:10.1029/2006TC002090.

Nishimura, S., and M. Hashimoto (2006), A model with rigid rotations and slip deficits for the GPS-derived velocity field in Southwest Japan, *Tectonophysics*, *421*, 187–207, doi:10.1016/j.tecto.2006.04.017.

Norabuena, E., et al. (2004), Geodetic and seismic constraints on some seismogenic zone processes in Costa Rica, *J. Geophys. Res.*, *109*, B11403, doi:10.1029/2003JB002931.

Obara, K. (2002), Nonvolcanic deep tremor associated with subduction in southwest Japan, *Science*, *296*, 1679–1681, doi:10.1126/science.1070378.

Obara, K., H. Hirose, F. Yamamizu, and K. Kasahara (2004), Episodic slow slip events accompanied by non-volcanic tremors in southwest Japan subduction zone, *Geophys. Res. Lett.*, *31*, L23602, doi:10.1029/2004GL020848.

Ohta, Y., F. Kimata, and T. Sagiya (2004), Reexamination of the interplate coupling in the Tokai region, central Japan, based on the GPS data in 1997–2002, *Geophys. Res. Lett.*, *31*, L24604, doi:10.1029/2004GL021404.

Ohta, Y., J. T. Freymueller, S. Hreinsdottir, and H. Suito (2006), A large slow slip event and the depth of the seismogenic zone in the south central Alaska subduction zone, *Earth Planet. Sci. Lett.*, *247*, 108–116, doi:10.1016/j.epsl.2006.05.013.

Okal, E. A. (1988), Seismic parameters controlling far-field tsunami amplitudes: A review, *Nat. Hazards*, *1*, 67–96, doi:10.1007/BF00168222.

Oleskevich, D. A., R. D. Hyndman, and K. Wang (1999), The updip and downdip limits to great subduction earthquakes: Thermal and structural models of Cascadia, south Alaska, SW Japan, and Chile, *J. Geophys. Res.*, *104*, 14,965–14,991, doi:10.1029/1999JB900060.

Ota, Y., K. R. Berryman, L. J. Brown, and K. Kashima (1989), Holocene sediments and vertical tectonic downwarping near Wairoa, northern Hawke's Bay, New Zealand, *N. Z. J. Geol. Geophys.*, *32*(3), 333–341.

Ota, Y., T. Miyauchi, and A. G. Hull (1990), Holocene marine terraces at Aramoana and Pourerere, eastern North Island, New Zealand, *N. Z. J. Geol. Geophys.*, *33*, 541–546.

Ota, Y., A. G. Hull, and K. R. Berryman (1991), Coseismic uplift of Holocene marine terraces in the Pakarae River area, Eastern North Island, New Zealand, *Quat. Res.*, *35*, 331–346, doi:10.1016/0033-5894(91)90049-B.

Ota, Y., A. G. Hull, N. Iso, Y. Ikeda, I. Moriya, and T. Yoshikawa (1992), Holocene marine terraces on the northeast coast of North Island, New Zealand, and their tectonic significance, *N. Z. J. Geol. Geophys.*, *35*, 273–288.

Ozawa, S., M. Murakami, M. Kaidzu, T. Tada, Y. Hatanaka, H. Yarai, and T. Nishimura (2002), Detection and monitoring of ongoing aseismic slip in the Tokai region, central Japan, *Science*, *298*, 1009–1012, doi:10.1126/science.1076780.

Pacheco, J. F., L. Sykes, and C. H. Scholz (1993), Nature of seismic coupling along simple plate boundaries of the subduction type, *J. Geophys. Res.*, *98*, 14,133–14,159, doi:10.1029/93JB00349.

Page, M. J., and N. A. Trustrum (1997), A late Holocene lake record of the erosion response to land use change in a steepland catchment, New Zealand, *Z. Geomorphol.*, *41*(3), 369–392.

Peacock, S. M., and R. D. Hyndman (1999), Hydrous minerals in the mantle wedge and the maximum depth of subduction thrust earthquakes, *Geophys. Res. Lett.*, *26*(16), 2517–2520, doi:10.1029/1999GL900558.

Pelayo, A. M., and D. A. Wiens (1992), Tsunami earthquakes: Slow thrust-faulting events in the accretionary wedge, *J. Geophys. Res.*, *97*, 15,321–15,337, doi:10.1029/92JB01305.

Peterson, E. T., and T. Seno (1984), Factors affecting seismic moment release rates in subduction zones, *J. Geophys. Res.*, *89*, 10,233–10,248, doi:10.1029/JB089iB12p10233.

Price, R. C., J. A. Gamble, I. E. M. Smith, R. B. Stewart, S. Eggins, and I. C. Wright (2005), An integrated model for the temporal evolution of andesites and rhyolites and crustal development in NZ's North Island, *J. Volcanol. Geotherm. Res.*, *140*, 1–24, doi:10.1016/j.jvolgeores.2004.07.013.

Ranero, C. R., and R. von Huene (2000), Subduction erosion along the Middle America convergent margin, *Nature*, *404*, 748–752, doi:10.1038/35008046.

Reyners, M. (1998), Plate coupling and the hazard of large subduction thrust earthquakes at the Hikurangi subduction zone, New Zealand, *N. Z. J. Geol. Geophys.*, *41*, 343–354.

Reyners, M. E. (2000), Quantifying the hazard of large subduction thrust earthquakes in Hawke's Bay, *Bull. N. Z. Soc. Earthquake Eng.*, *33*(4), 477–483.

Reyners, M., and S. Bannister (2007), Earthquakes triggered by slow slip at the plate interface in the Hikurangi subduction zone, New Zealand, *Geophys. Res. Lett.*, *34*, L14305, doi:10.1029/2007GL030511.

Reyners, M., and H. Cowan (1993), The transition from subduction to continental collision: Crustal structure in the North Canterbury region, New Zealand, *Geophys. J. Int.*, *115*, 1124–1136, doi:10.1111/j.1365-246X.1993.tb01514.x.

Reyners, M., and D. Eberhart-Phillips (2009), Small earthquakes provide insight into plate coupling and fluid distribution in the Hikurangi subduction zone, New Zealand, *Earth Planet. Sci. Lett.*, *282*(1–4), 299–305, doi:10.1016/j.epsl.2009.03.034.

Reyners, M., and P. McGinty (1999), Shallow subduction tectonics in the Raukumara Peninsula, New Zealand, as illuminated by earthquake focal mechanisms, *J. Geophys. Res.*, *104*(B2), 3025–3034, doi:10.1029/1998JB900081.

Reyners, M. E., P. McGinty, J. Ansell, and B. G. Ferris (1997a), The Tikokino earthquake of 11 April 1993: Movement at the plate interface in Southern Hawke's Bay, *Bull. N. Z. Soc. Earthquake Eng.*, *30*(3), 242–251.

Reyners, M., R. Robinson, and P. McGinty (1997b), Plate coupling in the northern South Island and southernmost North Island, New Zealand, as illuminated by earthquake focal mechanisms, *J. Geophys. Res.*, *102*(B7), 15,197–15,210, doi:10.1029/97JB00973.

Reyners, M., D. Eberhart-Phillips, and G. Stuart (1999), A three-dimensional image of shallow subduction: Crustal structure of the Raukumara Peninsula, New Zealand, *Geophys. J. Int.*, *137*(3), 873–890, doi:10.1046/j.1365-246x.1999.00842.x.

Reyners, M., D. Eberhart-Phillips, G. Stuart, and Y. Nishimura (2006), Imaging subduction from the trench to 300 km depth beneath the central North island, New Zealand, with Vp and Vp/Vs, *Geophys. J. Int.*, *165*, 565–583, doi:10.1111/j.1365-246X.2006.02897.x.

Rogers, G., and H. Dragert (2003), Episodic tremor and slip on the Cascadia subduction zone: The chatter of silent slip, *Science*, *300*, 1942–1943, doi:10.1126/science.1084783.

Rubin, A. M. (2008), Episodic slow slip events and rate-and-state friction, *J. Geophys. Res.*, *113*, B11414, doi:10.1029/2008JB005642.

Ruff, L. J. (1989), Do trench sediments affect great earthquake occurrence in subduction zones, *Pure Appl. Geophys.*, *129*(1–2), 263–282, doi:10.1007/BF00874629.

Ruff, L., and H. Kanamori (1980), Seismicity and the subduction process, *Phys. Earth Planet. Inter.*, *23*, 240–252, doi:10.1016/0031-9201(80)90117-X.

Ruff, L., and B. Tichelaar (1996), What controls the seismogenic plate interface in subduction zones?, in *Subduction Top to Bottom*, *Geophys. Monogr. Ser.*, vol. 96, edited by G. E. Bebout et al., pp. 105–111, AGU, Washington, D. C.

Saffer, D. M. (2003), Pore pressure development and progressive dewatering in underthrust sediments at the Costa Rican subduction margin: Comparison with northern Barbados and Nankai, *J. Geophys. Res.*, *108*(B5), 2261, doi:10.1029/2002JB001787.

Saffer, D. M., and B. A. Bekins (2006), An evaluation of factors influencing pore pressure in accretionary complexes: Implications for taper angle and wedge mechanics, *J. Geophys. Res.*, *111*, B04101, doi:10.1029/2005JB003990.

Satake, K., and Y. Tanioka (1999), Sources of tsunami and tsunamigenic earthquakes in subduction zones, *Pure Appl. Geophys.*, *154*, 467–483, doi:10.1007/s000240050240.

Savage, J. (1983), A dislocation model of strain accumulation and release at a subduction zone, *J. Geophys. Res.*, *88*(B6), 4984–4996, doi:10.1029/JB088iB06p04984.

Scholz, C. H. (1990), *The Mechanics of Earthquakes and Faulting*, 439 pp., Cambridge Univ. Press, New York.

Scholz, C. H. (1998), Earthquakes and friction laws, *Nature*, *391*, 37–42, doi:10.1038/34097.

Scholz, C. H., and J. Campos (1995), On the mechanism of seismic decoupling and back arc spreading at subduction zones, *J. Geophys. Res.*, *100*(B11), 22,103–22,116, doi:10.1029/95JB01869.

Scholz, C. H., and C. Small (1997), The effect of seamount subduction on seismic coupling, *Geology*, *25*(6), 487–490, doi:10.1130/0091-7613(1997)025<0487:TEOSSO>2.3.CO;2.

Segall, P., and J. Rice (1995), Dilatancy, compaction, and slip instability of a fluid-infiltrated fault, *J. Geophys. Res.*, *100*(B11), 22,155–22,171, doi:10.1029/95JB02403.

Sibson, R. H. (1984), Roughness at the base of the seismogenic zone: Contributing factors, *J. Geophys. Res.*, *89*, 5791–5799, doi:10.1029/JB089iB07p05791.

Sibson, R. H. (1992), Fault-valve behaviour and the hydrostatic-lithostatic fluid pressure interface, *Earth Sci. Rev.*, *32*, 141–144, doi:10.1016/0012-8252(92)90019-P.

Sibson, R. H., and J. V. Rowland (2003), Stress, fluid pressure and structural permeability in seismogenic crust, North Island, New Zealand, *Geophys. J. Int.*, *154*, 584–594, doi:10.1046/j.1365-246X.2003.01965.x.

Spinelli, G. A., and D. Saffer (2004), Along-strike variations in underthrust sediment dewatering on the Nicoya margin, Costa Rica related to the updip limit of seismicity, *Geophys. Res. Lett.*, *31*, L04613, doi:10.1029/2003GL018863.

Stein, S., and E. A. Okal (2007), Ultralong period seismic study of the December 2004 Indian Ocean earthquake and Implications for regional tectonics and the subduction process, *Bull. Seismol. Soc. Am.*, *97*, S279–S295, doi:10.1785/0120050617.

Stern, T. A., and F. J. Davey (1990), Deep seismic expression of a foreland basin: Taranaki Basin, New Zealand, *Geology*, *18*, 979–982, doi:10.1130/0091-7613(1990)018<0979:DSEOAF>2.3.CO;2.

Stern, T. A., W. R. Stratford, and M. L. Salmon (2006), Subduction evolution and mantle dynamics at a continental margin: Central North Island, New Zealand, *Rev. Geophys.*, *44*, RG4002, doi:10.1029/2005RG000171.

Subarya, C., M. Chlieh, L. Prawirodirdjo, J.-P. Avouac, Y. Bock, K. Sieh, A. J. Meltzner, D. H. Natawidjaja, and R. McCaffrey (2006), Plate-boundary deformation associated with the great Sumatra–Andaman earthquake, *Nature*, *440*(7080), 46–51, doi:10.1038/nature04522.

Suwa, Y., S. Miura, A. Hasegawa, T. Sato, and K. Tachibana (2006), Interplate coupling beneath NE Japan inferred from three-dimensional displacement field, *J. Geophys. Res.*, *111*, B04402, doi:10.1029/2004JB003203.

Tanioka, Y., L. Ruff, and K. Satake (1997), What controls the lateral variation of large earthquake occurrence along the Japan Trench?, *Isl. Arc*, *6*, 261–266, doi:10.1111/j.1440-1738.1997.tb00176.x.

Taylor, B. (2006), The single largest oceanic plateau: Ontong Java-Manihiki-Hikurangi, *Earth Planet. Sci. Lett.*, *241*, 372–380, doi:10.1016/j.epsl.2005.11.049.

Thatcher, W. (1990), Order and diversity in the modes of circum-Pacific earthquake recurrence, *J. Geophys. Res.*, *95*, 2609–2623, doi:10.1029/JB095iB03p02609.

Tichelaar, B., and L. J. Ruff (1993), Depth of seismic coupling along subduction zones, *J. Geophys. Res.*, *98*, 2017–2037, doi:10.1029/92JB02045.

Townend, J. (1997), Subducting a sponge; minimum estimates of the fluid budget of the Hikurangi Margin accretionary prism, *Geol. Soc. N. Z. Newsl.*, *112*, 14–16.

Tse, S. T., and J. R. Rice (1986), Crustal earthquake instability in relation to the depth variation of frictional slip properties, *J. Geophys. Res.*, *91*, 9452–9472, doi:10.1029/JB091iB09p09452.

Uyeda, S., and H. Kanamori (1979), Back-arc opening and the mode of subduction, *J. Geophys. Res.*, *84*, 1049–1061, doi:10.1029/JB084iB03p01049.

von Huene, R., C. R. Ranero, and P. Vannucchi (2004), A generic model of subduction erosion, *Geology*, *32*, 913–916, doi:10.1130/G20563.1.

Vrolijk, P. (1990), On the mechanical role of smectite in subduction zones, *Geology*, *18*, 703–707, doi:10.1130/0091-7613(1990)018<0703:OTMROS>2.3.CO;2.

Walcott, R. I. (1984), The kinematics of the plate boundary zone through New Zealand: A comparison of short and long-term deformation, *Geophys. J. R. Astron. Soc.*, *79*, 613–633.

Walcott, R. I. (1987), Geodetic strain and the deformational history of the North Island of New Zealand during the late Cainozoic, *Philos. Trans. R. Soc. London, Ser. A*, *321*, 163–181, doi:10.1098/rsta.1987.0009.

Wallace, L. M., and R. J. Beavan (2006), A large slow slip event on the central Hikurangi subduction interface beneath the Manawatu region, North Island, New Zealand, *Geophys. Res. Lett.*, *33*, L11301, doi:10.1029/2006GL026009.

Wallace, L. M., J. Beavan, R. McCaffrey, and D. Darby (2004), Subduction zone coupling and tectonic block rotations in the North Island, New Zealand, *J. Geophys. Res.*, *109*, B12406, doi:10.1029/2004JB003241.

Wallace, L. M., S. Ellis, K. Miyao, S. Miura, J. Beavan, and J. Goto (2009), Enigmatic, highly active left-lateral shear zone in southwest Japan explained by aseismic ridge collision, *Geology*, *37*(2), 143–146, doi:10.1130/G25221A.1.

Wang, K., and T. Dixon (2004), "Coupling" semantics and science in earthquake research, *Eos Trans. AGU*, *85*(18), 180.

Wang, K., and Y. Hu (2006), Accretionary prisms in subduction earthquake cycles: The theory of dynamic Coulomb wedge, *J. Geophys. Res.*, *111*, B06410, doi:10.1029/2005JB004094.

Wang, K., and K. Suyehiro (1999), How does plate coupling affect crustal stresses in Northeast and Southwest Japan?, *Geophys. Res. Lett.*, *26*(15), 2307–2310, doi:10.1029/1999GL900528.

Webb, T., and H. Anderson (1998), Focal mechanisms of large earthquakes in the North island of New Zealand: Slip partitioning at an oblique active margin, *Geophys. J. Int.*, *134*, 40–86, doi:10.1046/j.1365-246x.1998.00531.x.

Wilson, C. J. N., B. F. Houghton, M. O. McWilliams, M. A. Lanphere, S. D. Weaver, and R. M. Briggs (1995), Volcanic and structural evolution of Taupo Volcanic Zone, New Zealand: A review, *J. Volcanol. Geotherm. Res.*, *68*, 1–28, doi:10.1016/0377-0273(95)00006-G.

Wilson, K., K. R. Berryman, N. Litchfield, and T. Little (2006), A revision of mid-late Holocene marine terrace distribution and chronology at the Pakarae River mouth, North Island, New Zealand, *N. Z. J. Geol. Geophys.*, *49*, 477–489.

Wilson, K. J., K. Berryman, U. Cochran, and T. Little (2007), Early Holocene paleoseismic history at the Pakarae locality, eastern North Island, New Zealand, inferred from transgressive marine sequence architecture and biostratigraphy, *Tectonics*, *26*, TC4013, doi:10.1029/2006TC002021.

Winkler, K. W., and W. F. Murphy (1994), Acoustic velocity and attenuation in porous rocks, in *Rock Physics and Phase Relations: A Handbook of Physical Constants*, *AGU Ref. Shelf*, vol. 3, edited by T. J. Ahrens, pp. 20–34, AGU, Washington, D. C.

Yamanaka, Y., and M. Kikuchi (2004), Asperity map along the subduction zone in northeastern Japan inferred from regional seismic data, *J. Geophys. Res.*, *109*, B07307, doi:10.1029/2003JB002683.

Zoback, M., R. Jachens, and J. Olson (1999), Abrupt along-strike change in tectonic style: San Andreas fault zone, San Francisco Peninsula, *J. Geophys. Res.*, *104*(B5), 10,719–10,742, doi:10.1029/1998JB900059.